NASA Contractor Report 158957

EXPERIMENTS ON TANDEM DIFFUSERS WITH BOUNDARY-LAYER SUCTION APPLIED IN BETWEEN

P. Stephen Barna

OLD DOMINION UNIVERSITY RESEARCH FOUNDATION
Norfolk, Virginia 23508

NASA Contract NAS1-14193-Tasks 6 and 42
February 1979

National Aeronautics and
Space Administration

Langley Research Center
Hampton, Virginia 23665

TABLE OF CONTENTS

LIST OF FIGURES

(Continued)

LIST OF FIGURES (Concl'd)

EXPERIMENTS ON TANDEM DIFFUSERS WITH BOUNDARY-LAYER SUCTION APPLIED IN BETWEEN

By

P. Stephen Barna

ABSTRACT

Experiments were performed on conical diffusers of various configurations with the same, but rather unusually large, 16:1 area ratio. Because available performance data on diffusers fall short of very large area ratio configurations, an unconventional design, consisting of two diffusers following each other in tandem, was proposed. Both diffusers had the same area ratio of 4:1, but had different taper angles. While for the first diffuser (called "leading") the angle remained constant, for the second (called "follower"), the taper angle was stepped up to higher values. Boundary-layer control, by way of suction, was applied between the diffusers, and a single slot suction ring was inserted between them. The leading diffuser had an enclosed nominal divergence angle 2θ = 5 degrees, while the follower diffusers had either 10, 20, 30, or 40 degrees, respectively, giving 4 combinations.

The experiments were performed at four different Reynolds numbers and with various suction rates. The results indicate a general improvement in the performance of all diffusers with boundary-layer suction. It appears that the improvement of the pressure recovery depends on both the Reynolds number and the suction rate, and the largest increase, 0.075, was found at the lowest R_e when the follower divergence was 2θ = 40 degrees. It also appears, however, that the rate of suction as compared with the flow rate through the diffuser must be relatively high; thus, the suction power necessary for effective improvements becomes also rather large, so that the benefit in improving diffuser performance by suction may be partly offset by power requirements.

INTRODUCTION

The idea of employing boundary-layer control by way of suction is certainly not new, and results of various investigations in the literature (refs. 1 to 5) show promise of improved pressure recovery when suction is applied either at the diffuser inlet or at some location downstream from the inlet. The beneficial effects of suction at the inlet on performance are of course known to be due to the decreased blockage, which has been found to be one of the major factors affecting pressure recovery. It may also be considered rational to control the layer at some location downstream from the inlet by way of suction or other means (ref. 6), but the exact location where this should be applied becomes more problematical. It has been suggested that control, especially suction, should be applied at a location which is just upstream from the point of separation. This point may be too far downstream. Furthermore, a problem arises in locating this point where the flow would be expected to separate because the point of separation is known to depend on various factors, such as the "history" of the flow (blockage), the Reynolds number, the turbulence level, and so on, which are not always available to the designer.

Fortunately, the designer of "conventional" (conical or flat straight-wall) diffusers can obtain adequate information (ref. 7) from systematic parametric experimental studies. The designer, however, would face difficulties when called upon to furnish an equally efficient but unconventional design. To the category of unconventional designs belong the "short" diffusers and the "large-area-ratio" designs. Because straight-walled diffusers of the conventional design require long spaces due to their recommended low divergence angle, increasing attention is being paid to the practice of enlarging the divergence angle and thus reducing the length. The shortening of a single, straight-walled diffuser, however, invariably leads to larger losses as well as to severe velocity fluctuations at exit, which at times (as in the case of wind tunnels) are most undesirable. In addition, the velocity profile tends to become distorted, that is, less full in comparison with the fully developed turbulent flow velocity distribution, characteristic of flow in parallel pipes. This is bound to remain so, even if the boundary layer starts with zero thickness due to its removal by suction at the inlet to the diffuser.

The author of this paper proposes a conventional, low-taper, straight-walled, high-efficiency diffuser as a means to start pressure recovery of a certain flow, which is to be followed by a second straight-walled diffuser with a larger taper angle. In order to render the second diffuser more efficient, boundary-layer control is also proposed at the cross-sectional area where the second diffuser joins the first. Such a setup may be considered a "tandem" configuration, and it is convenient to call the first diffuser the "leading" and the second the "follower." Straight-walled diffusers may be considered less difficult to make than continuous curved-wall designs, which have been the subject of studies by various authors. Admittedly, there must be an infinite variety of combinations in designing tandem diffusers, and it is of interest to see the comparative length of a diffuser with an area ratio of 16:1 consisting of two diffusers in tandem, each having an area ratio of 4:1. Figure 1 shows a set of tandem diffusers with the same leading diffuser combined with four different followers with larger divergence angles, and their overall length is compared with a single-taper straight diffuser.

It appears that the overall length decreases rapidly with increasing follower divergence angle, and one may notice the marked decrease in overall length from the single-taper "original" diffuser with $2\theta = 5$ degree divergence to a diffuser in which the divergence of the follower is increased to $2\theta = 10$ degrees. A space saving of 34.4 percent results! A further increase in divergence to $2\theta = 20$ degrees halves the overall length of the original single-taper diffuser a space saving of 50 percent! Any further increase in the follower taper, however, only results in smaller decreases which then may be considered less significant.

Tandem diffusers may find application in wind tunnels where the large space requirement is generally due to the long diffuser's following the working section. While the power required to provide the necessary suction may add to the initial and operating costs of the tunnel, the saving of building space, construction cost, and land price may lead to a favorable consideration of this proposal.

SYMBOLS

A	cross-sectional area
a	acoustic speed of air (346 m/s)
B	blockage due to displacement by boundary layer
C_p	pressure recovery coefficient
D	diameter
H	shape parameter
L	diffuser centerline length
M_c	Mach number at centerline, defined as U_c/a
p_t	static pressure at diffuser inlet
p_e	static pressure at diffuser exit
q	volumetric flow rate of suction
Q	volumetric flow rate of the main flow through the diffuser at inlet
q/Q	normalized suction rate
R_1	radius of inlet pipe
R_e	Reynolds number
T_1	traverse plane at inlet
T_2	traverse plane ahead of suction ring
T_3	traverse plane immediately downstream from the ring
T_4	traverse plane at exit from the diffuser
u	velocity at some distance y from the wall
U_c	velocity at centerline (also U_{max})
y	distance from the wall
δ^*	boundary-layer displacement thickness
δ^{**}	boundary-layer momentum thickness
θ	diffuser taper angle

2θ diffuser divergence angle

ρ air density

ν kinematic viscosity of air

Subscripts

e exit plane

1 inlet plane

c center line

PERFORMANCE PARAMETERS

Diffuser performance in the form of "pressure recovery" is given by the coefficient

$$C_p = \frac{P_e - p_1}{\frac{1}{2}\rho U_c^2}$$

where the static pressure p is measured at the centerline, both at inlet and outlet

The Reynolds number was calculated by $R_e = U_c D_1/\nu$ where D_1 (or W_1) is the diameter at inlet

The blockage at inlet

$$B = 1 - \frac{A_{eff}}{A_{geom}}$$

where the effective area open to flow is considered the geometric area less the annular area $\pi D_1 \delta^*$ (See Appendix A).

For the circular pipe with thin boundary layer and symmetric velocity distribution, the displacement thickness is given by

$$\delta^* = \int_o^R \left(1 - \frac{u}{U_c}\right)\left(1 - \frac{y}{R}\right) dy$$

and the momentum thickness is given by

$$\delta^{**} = \int_0^R \frac{u}{U_c}\left(1 - \frac{u}{U_c}\right)\left(1 - \frac{y}{R}\right) dy$$

(See Appendix B).

The shape parameter is defined as

$$H = \frac{\delta^*}{\delta^{**}}$$

TEST SETUP

The test setup essentially consisted of an open air system taking in and discharging air into a large room A centrifugal air blower, driven by a 15 HP 4-speed electric motor, discharged into a settling tank through a diffuser. Air from the tank entered a parallel pipe which was followed by a smaller diameter, long, parallel, inlet pipe leading to the diffuser. Between these pipes a contraction was inserted which was employed to determine the main flow rate into the diffuser The leading diffuser was directly connected to the inlet pipe and had the same diameter as the pipe at its inlet (D_1) while the follower diffuser had a $2D_1$ diameter at inlet and a $4D_1$ diameter at exit. Finally, the air discharged into the surroundings through a short pipe of $6D_1$ length A suction ring was inserted between the exit of the leading diffuser and the inlet to the follower diffuser, and the bleed air from the suction ring was led through six plastic tubes to a collector chamber. A standard Venturi meter was employed to measure the suction rate, and a variable-speed centrifugal blower was used to create the necessary suction. The general arrangement of the test setup is shown in figure 2

The suction ring consisted of two parts. an annular chamber which was fastened to the leading diffuser and a cover plate which sealed the chamber. The two parts were separated by pads through which the bolts passed and the air was free to flow radially, first through the suction slot, then through the passages open to flow between the pads. Finally, the air was removed from the chamber through six equally spaced ports through which the air flowed into the

suction tubes. Details of the suction ring are shown in figure 3. Care was taken to ensure equal flow through each tube, and for this reason the tubes were cut to equal length and joined in a symmetrical pattern to the cylindrical collector chamber at their ends [see fig 2(b)]

Static pressure tappings were distributed with equal spacing along the diffusers to measure the pressure distribution, while the pressure difference between exit and inlet plane was measured at the centerline using standard pitot-static tubes with the static holes in alignment with the plane. The pitot tubes were also employed to take velocity traverses in these planes (shown as T_1 and T_4 in fig. 2) in addition to two other planes (shown as T_2 and T_3) located just upstream and downstream from the suction ring. Various liquid-in-tube manometers were employed to measure the pressure, using alcohol as the indicating fluid The velocity profiles in the upstream boundary layer were obtained with a special traverse mechanism capable of moving the probe 0.025 mm at a time. Figure 4 shows a cross-sectional view of the probes used for boundary-layer studies in the leading diffuser, and figure 2(d) shows the traverse mechanism.

Velocity profiles at exit were measured with time-averaging instruments because of the large fluctuations present in the stream All diffusers were made of galvanized steel of 16-gauge thickness while the suction ring was carefully machined from aluminum

TEST PROCEDURE

All experiments were performed with air under subsonic and steady-flow conditions. Pressure distributions and the kinetic head at inlet, $\frac{1}{2}\rho U_c^2$ (measured at the centerline), were photographically recorded from the manometer board. The main flow rate and the bleed air were measured with separate manometers of adequate sensitivity Each data point of the velocity profiles at traverse plane T_4 was averaged for 10 seconds.

Each test run consisted of: (a) selecting first the Reynolds number by setting the main blower speed control to a constant value, 1800, 1200, 900, or 600 revolutions per minute, and (b) by gradually varying the suction blower speed from 0 to a maximum in 8 separate steps, taking readings at each step. The procedure was repeated for the 4 different diffuser combinations, where the

fixed leading diffuser with 2θ = 5 degrees was joined to the follower diffuser of either 2θ = 10, 15, 20, 30, or 40 degrees. During all tests the ambient air conditions were carefully noted.

Because of the large amount of time necessary for taking velocity traverses, these were only taken for zero and maximum suction. The samples presented are considered adequate to represent a fair indication of the underlying phenomena.

TEST RESULTS

Pressure Recovery

Results of tests on pressure recovery are presented in figures 5 to 9. In particular, figures 5, 6, and 7 show the improvement in pressure recovery with increasing suction. These results can be presented in various ways or forms, each showing the same results in a different light.

Figure 5 shows the effect of suction on pressure recovery at constant Reynolds numbers for various diffuser followers, when C_p is plotted against normalized suction flow rate q/Q. This representation allows estimation of the suction rate q to be compared with the main flow rate Q. Since the amount of suction was limited by the power available to the suction blower, as the Reynolds number (and the main flow) was increased the q/Q maximum decreased. For example, at low Reynolds numbers about 60 percent was the maximum q/Q while at high Reynolds numbers only 19 percent was the maximum. The same results may be represented for one follower only by changing the Reynolds number with the variation of the main blower speed as shown in figure 6, where C_p is plotted against q/Q for four different blower speeds. Again, these results can be plotted using, this time, another normalized suction rate q/q_{max} where q_{max} is the maximum attainable suction rate that could be extracted from the flow for a given fixed main flow rate. The replotting of C_p makes it possible for the independent variable q/q_{max} to always end at the same value one, as shown in figure 7, where the lines tend to run parallel with each other.

It appears at once that recovery consistently increases with increasing suction. While in figures 5 and 6 the lines cross each other at times, they nearly run parallel with each other in figure 7 The inclination of the

lines with the horizontal ordinate is the largest at low Reynolds numbers for all follower diffusers, hence the improvement is the largest at low Reynolds numbers. However, the improvement in pressure recovery becomes progressively smaller with increasing Reynolds number.

Finally the results can be "cross-plotted" by employing diffuser angle as an independent variable as shown in figure 8. This representation also confirms that suction becomes less effective at higher Reynolds numbers. The effect of the Reynolds number on the recovery of the leading diffuser is shown in figure 9. It appears that recovery rapidly increases first (1.5 to 3.0 $\times$ 10^5) but shows little improvement at higher Reynolds numbers.

Velocity Distribution

Velocity distribution along the flow in both the leading diffuser and the 10° followers are shown in figures 10 and 11. These figures show how rapidly the velocity-profiles change. It appears from figure 10 that even in a low-taper diffuser (2θ $\approx$ 5°) the profiles deform more and more along the flow. The perfectly "normal" fully developed turbulent velocity profile at inlet (marked A) becomes gradually "peaked" while, at the exit (marked F), a large portion of the flow is displaced towards the center by the rapidly growing boundary layer along the diffuser wall The suction slot apparently trips the boundary layer because the flow entering the follower diffuser is found to some extent corrected as shown in figure 11 (a and b). At the inlet to the follower, application of suction results in a marked change in the velocity profile near the wall, but the shape changes little further away from the wall. However, further downstream from the suction slot, the velocity profiles at the wall become less and less affected by the suction, while near the center the profiles show improvement Hence the velocity profiles appear less "peaked" as shown in figures 11 (c to f).

The effect of the suction slot as a tripping device may also be observed from figure 12, where the boundary-layer shape parameter H is plotted against distance along the diffusers. While the value of H increases from 1.3 to 2.45 along the leading diffuser, it suddenly decreases to about 1.75 to 1.80 over a short distance regardless of suction. Along the follower, however, H first increases then decreases, again regardless of suction. This finding is rather unexpected considering the consistent rise in H

along the leading diffuser. Although H does not appear to rise above the value of 2.4 to 2.5, it cannot be stated with certainty that the flow may be considered unseparated. Blockage of the flow at the inlet to the leading diffuser at a low Reynolds number (1×10^5) was found to be about 17 percent, which decreased to about 11 percent when attaining $R_e = 5.9 \times 10^5$, as shown in figure 13. Details of calculations of the blockage are presented in Appendix A.

Effects of suction on the velocity profiles in the T_2, T_3, and T_4 planes are shown in figures 14, 15, and 16. It appears that, due to the effect of suction, the velocity across the T_2 plane slightly increases while a little further downstream at T_3 immediately downstream from the suction ring (fig. 15) the reverse effect is noticeable because the action of the suction slot as a sink affects the immediate surroundings as well as reducing the mass flow rate in the follower diffuser. Finally, the most marked effect of suction on velocity distribution appears at the exit plane (T_4) of the follower, and the change in profiles is shown in figure 16 for three followers.

Flow Stability

The effect of suction on flow stability was only studied to a limited extent. The absolute magnitudes of the velocity fluctuations at the centerline of the T_4 plane were automatically recorded by a readout amplifier connected to a pressure transducer A sample of such a record is shown in figure 17 where a marked reduction in amplitude was noticeable when suction was employed.

Local Pressure Distribution

Pressure distributions along the leading diffuser were recorded but because of space considerations are omitted from this report. A sample of pressure distribution along the flow in the 10° follower is shown in figure 18 It appears that suction improves the recovery of both the leading and the follower diffuser to about the same extent, although the reasons for this improvement may differ slightly The effect of suction manifests itself in a local pressure decrease where the suction ring is located which affects the leading diffuser by simply inducing more flow to pass through.

The resulting decrease in flow velocity lowers the pressure at the inlet where the velocity is highest so that the pressure difference increases, thus improving recovery in the leading diffuser. This is slightly offset by a corresponding increase in U_c at the suction ring resulting in some decrease in pressure. Since the follower discharges into the surroundings where atmospheric pressure is maintained, employing suction at inlet to follower diffuser improves recovery by the increase of pressure difference between inlet and exit and a decrease in dynamic head.

CONCLUSIONS

1 Diffusers employed in tandem can effectively reduce the overall length as compared to single straight-wall diffusers of the same initial divergence.

2. Results indicate that recovery of a wider angle diffuser provided with suction can favorably compare with the recovery of a lower taper diffuser without suction.

3. The amount of suction required to be effective in tandem diffusers appears to be larger than suction applied at the inlet of straight diffusers as found by some investigators.

4. Velocity distributions upstream from the suction slot are only slightly affected by the action of suction Immediately downstream from the slot, however, profile changes occur near the wall, while at exit, as a consequence of large suction rates, the centerline velocity decreases markedly, thus improving the velocity profile

5. The absolute magnitude of velocity fluctuations at exit from the follower diffuser can be markedly reduced by employing suction.

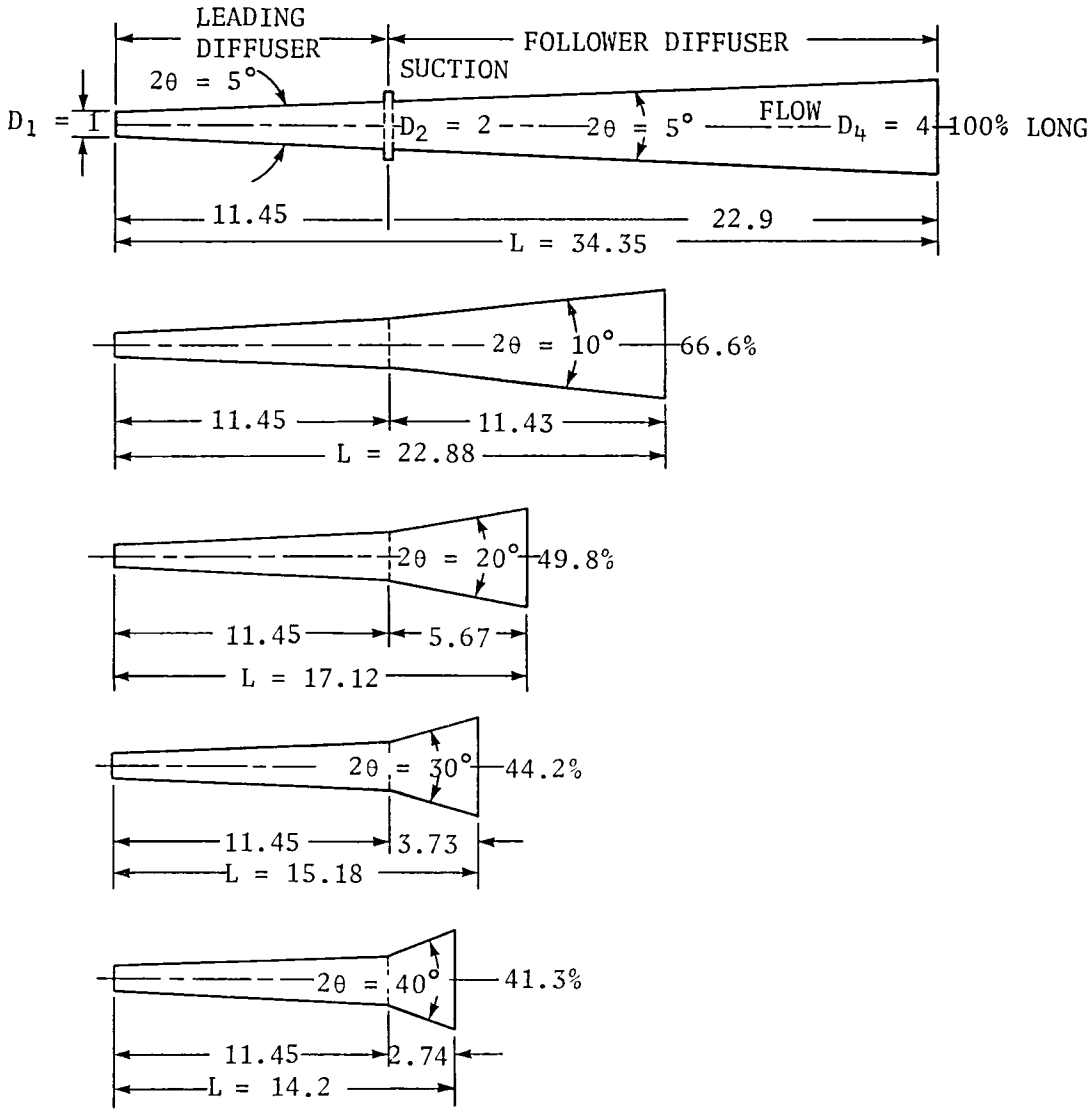

Figure 1. Proportions of tandem diffusers relative to inlet diameter D_1 with the followers assuming divergence 2θ = 5, 10, 20, 30, and 40 degrees.

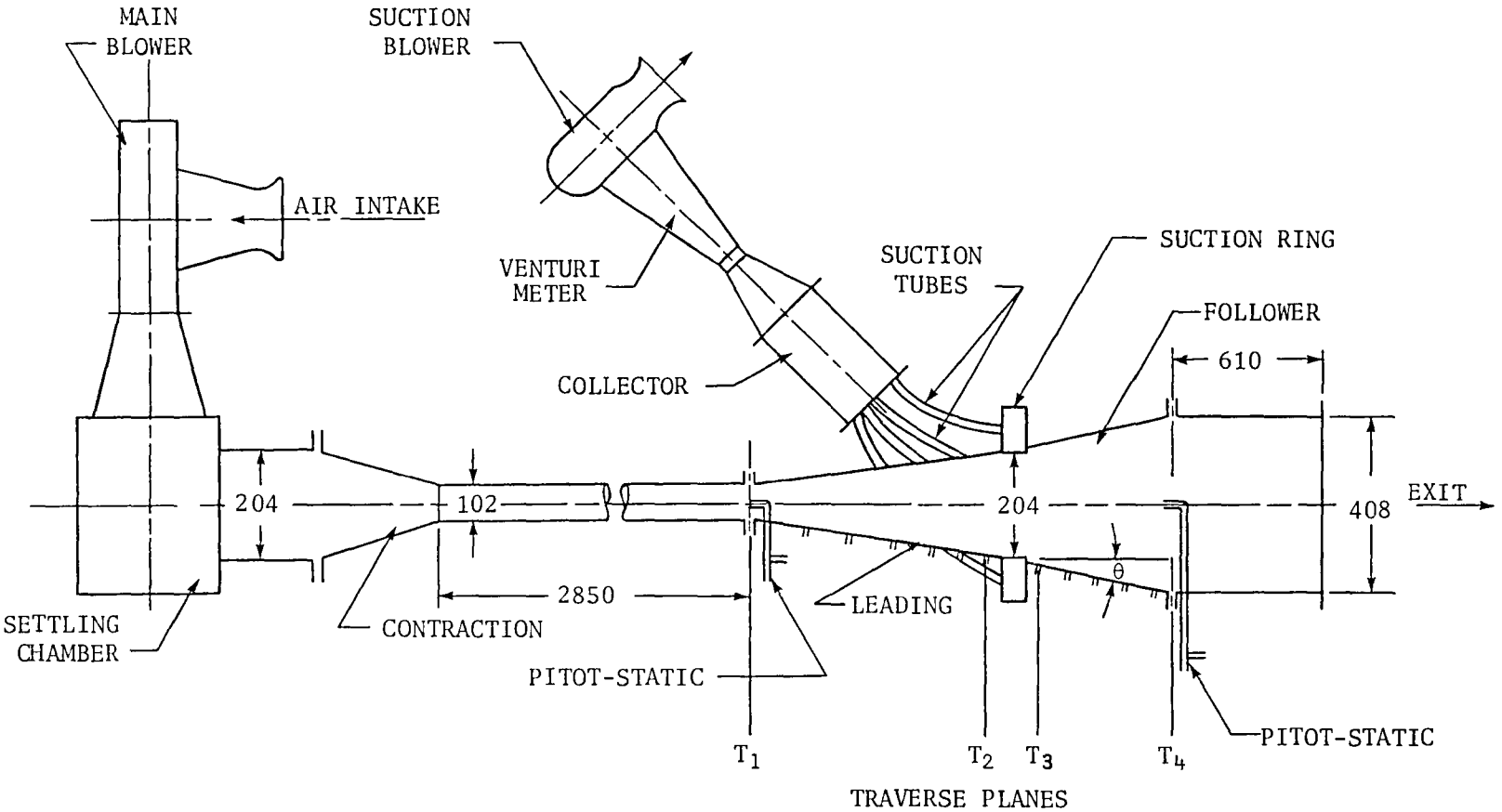

Figure 2(a). General arrangement of the test setup. (All dimensions in mm.)

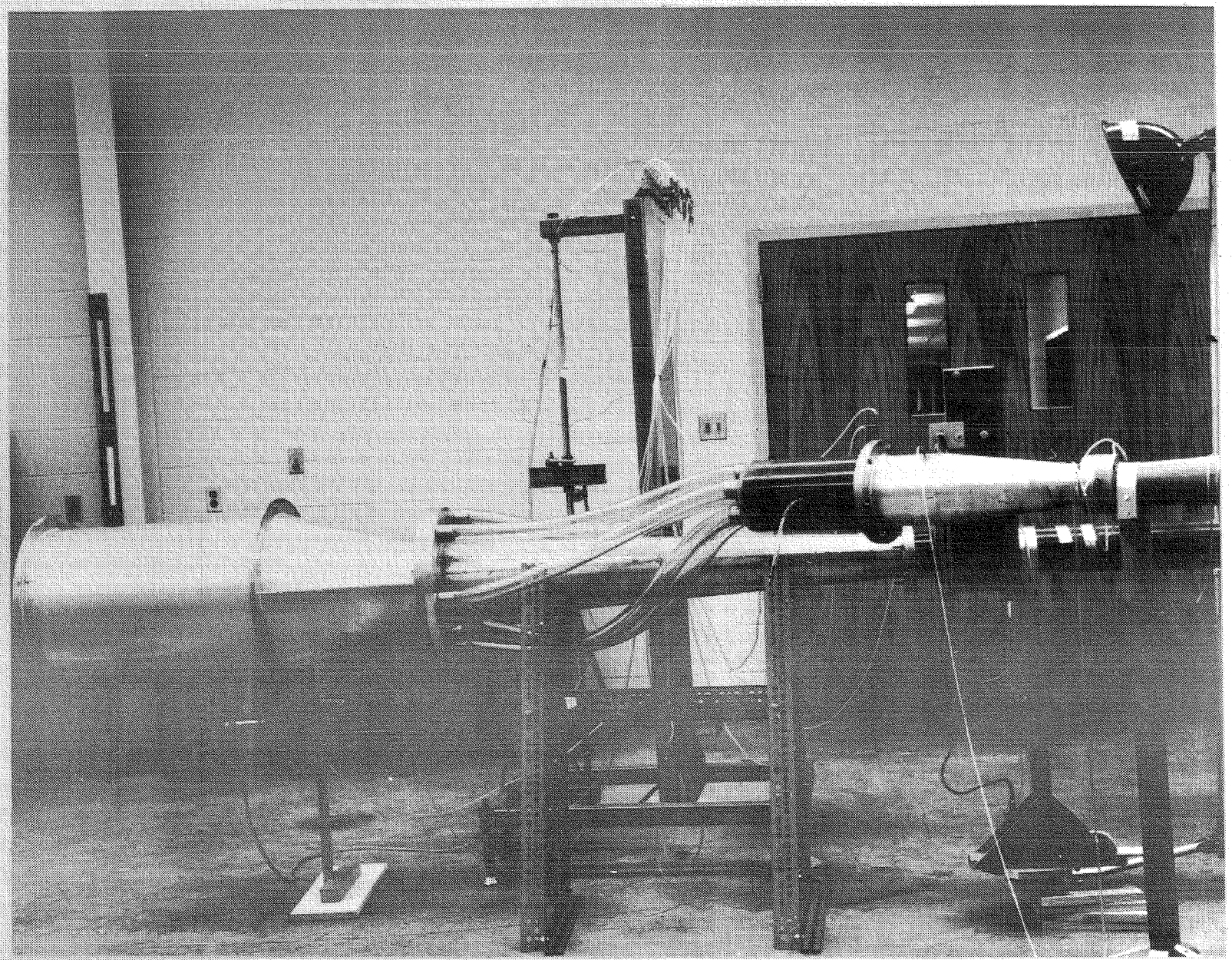

Figure 2(b). Detail of test setup showing leading suction ring and follower diffuser.

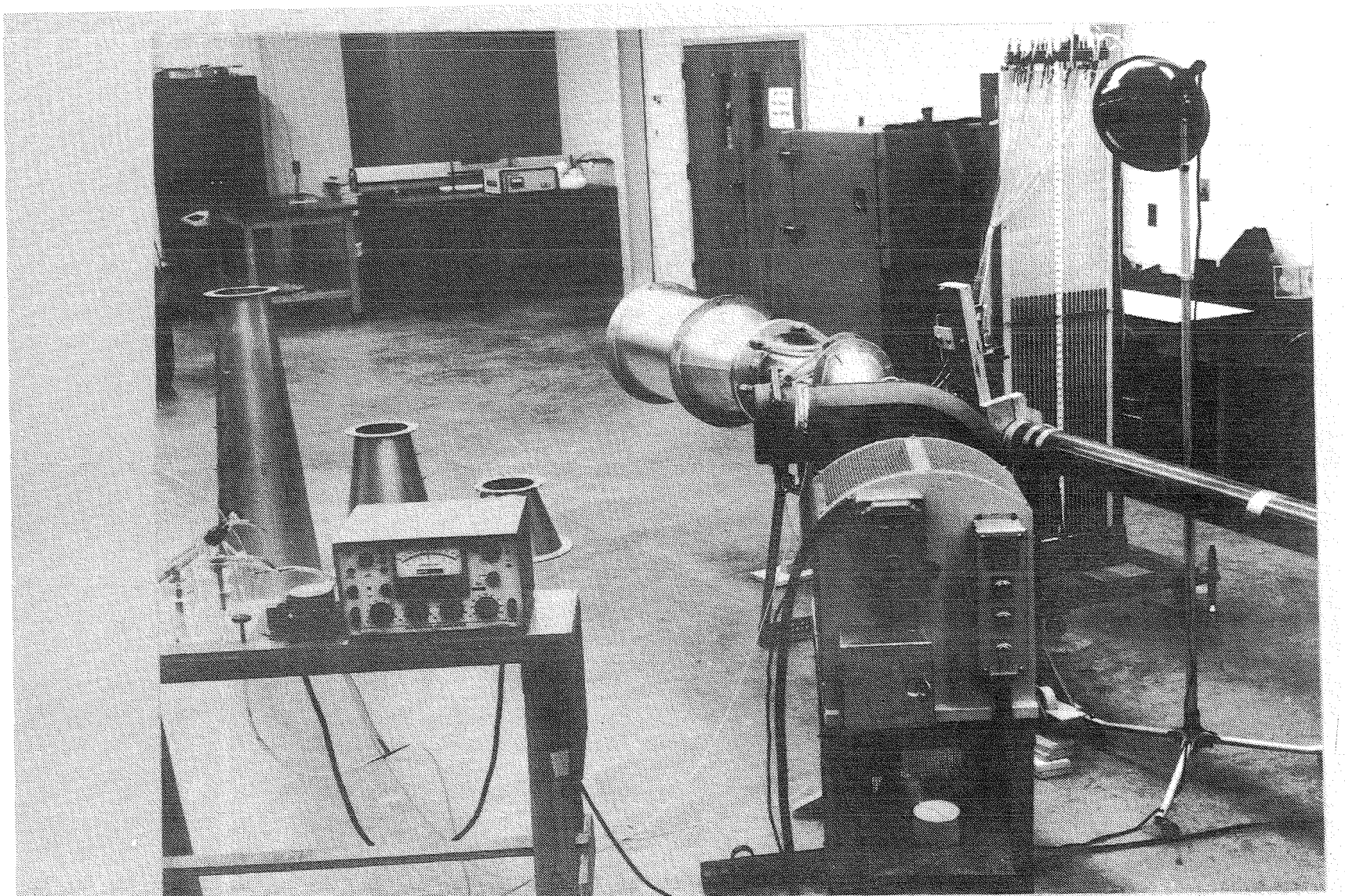

Figure 2(c). Detail of test setup showing various followers and suction fan.

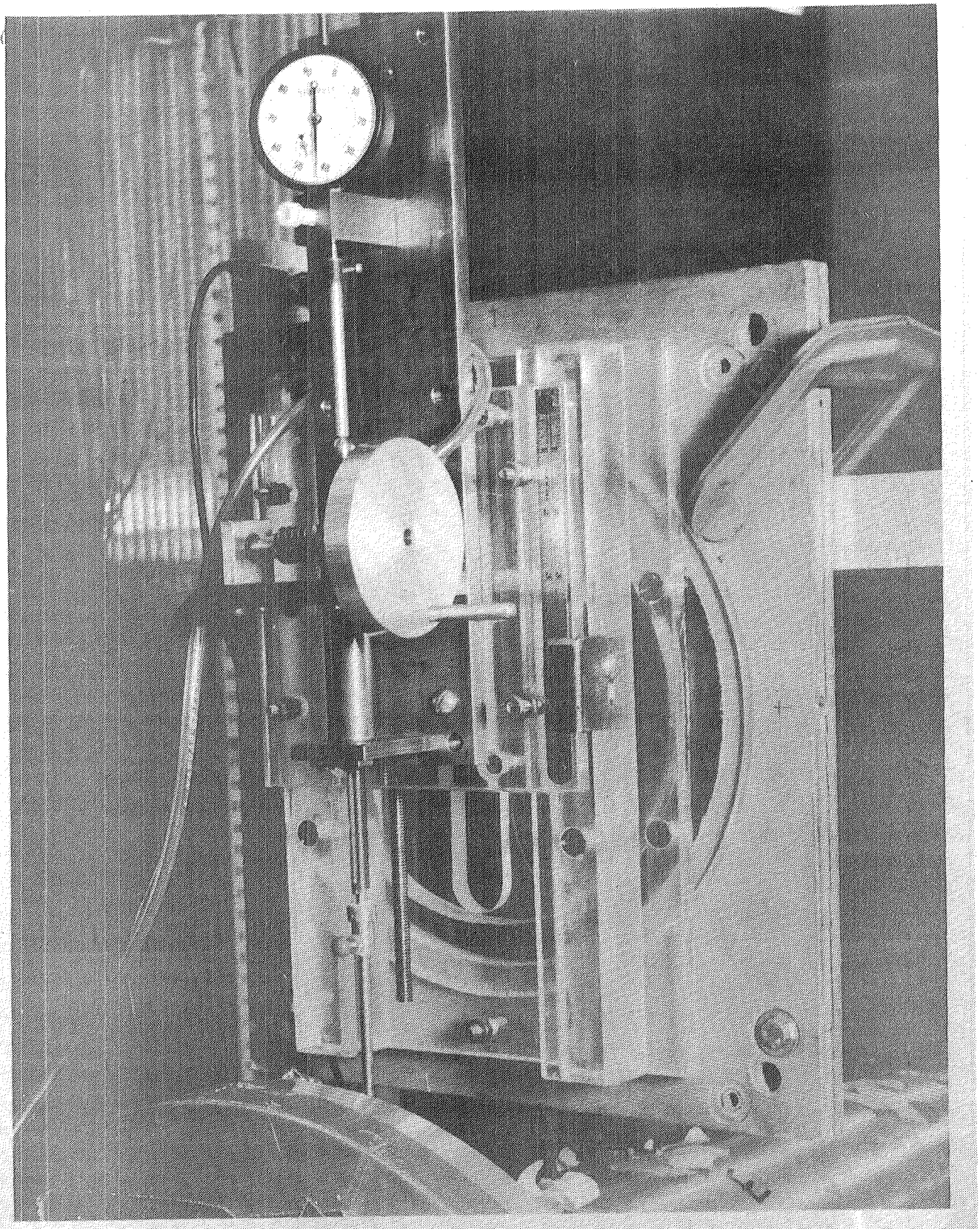

Figure 2(d). Detail showing boundary-layer traverse mechanism.

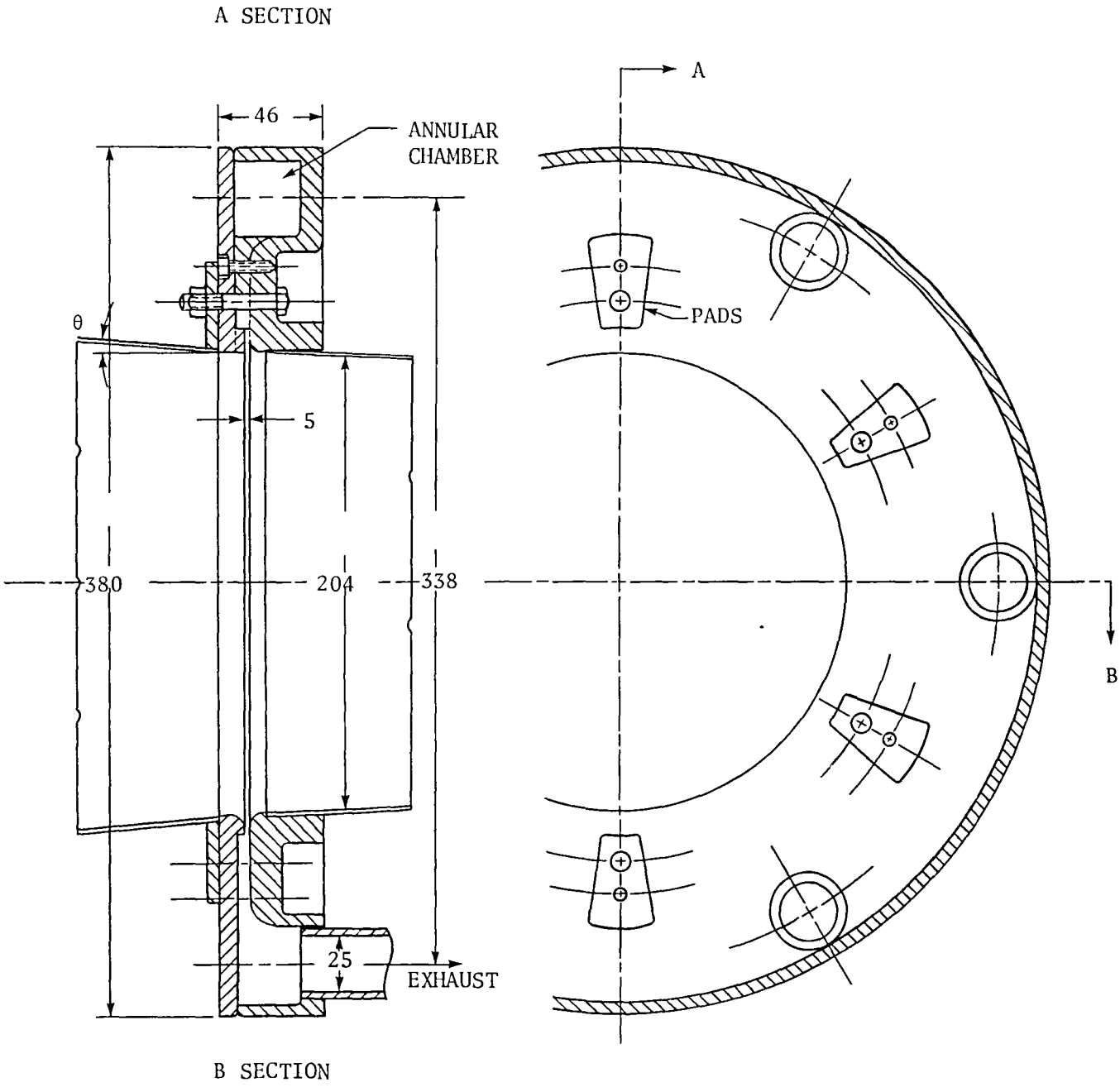

Figure 3. Detail of the suction ring.

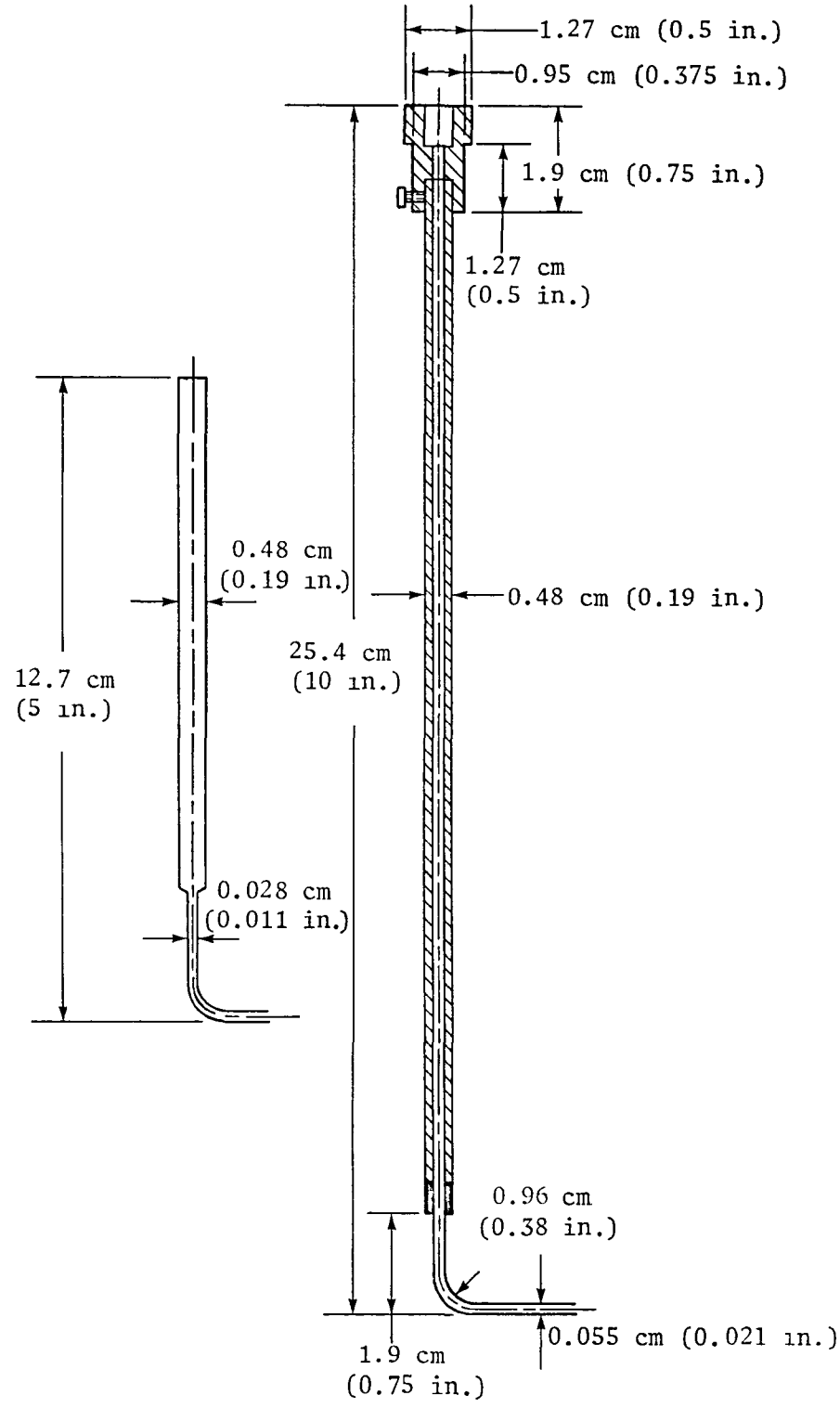

Figure 4. Probes for boundary-layer studies in leading diffuser.

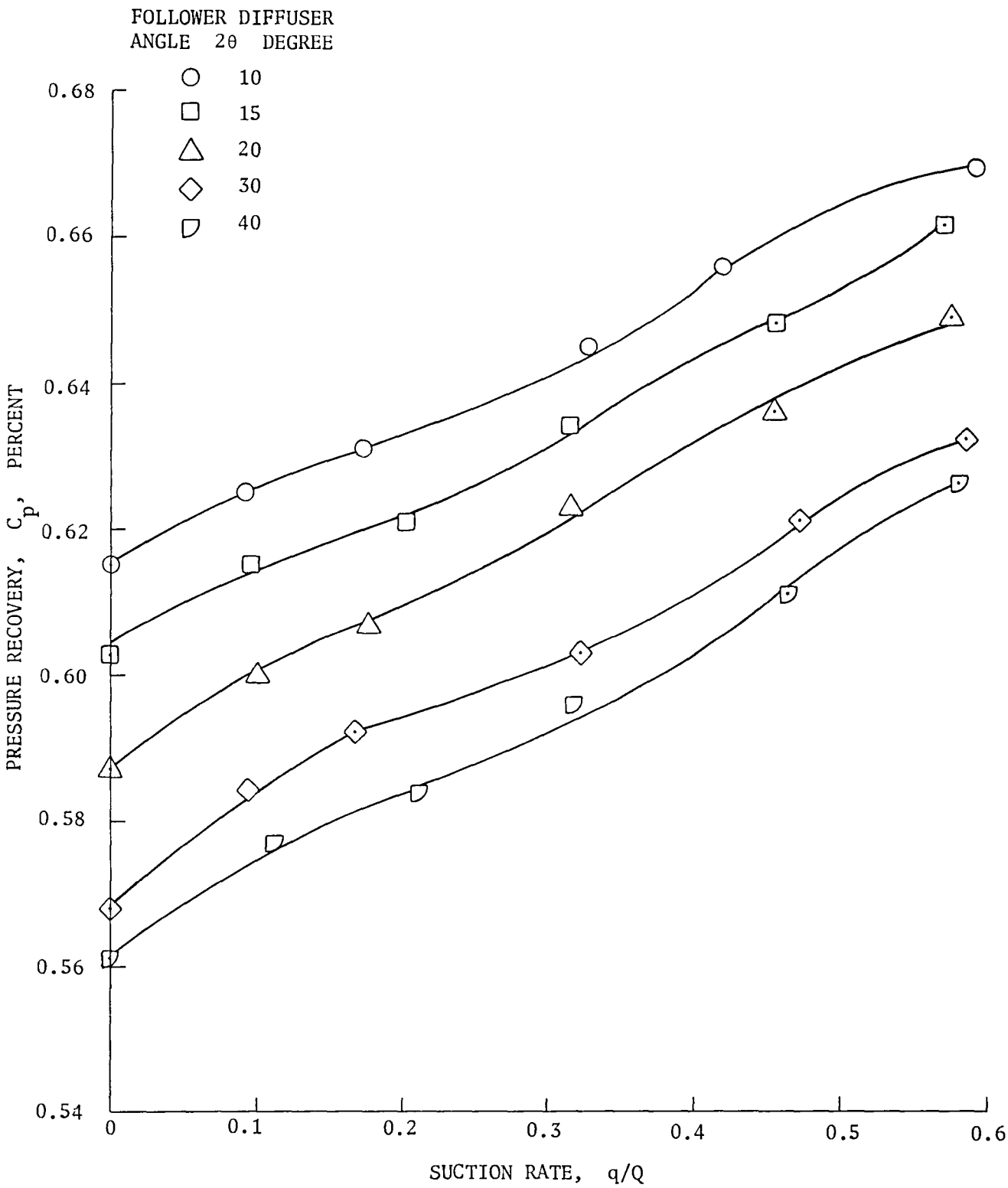

(a) Reynolds number $R_e = 1.86 \times 10^5$.

Figure 5. Effects of suction on pressure recovery at constant Reynolds numbers for various diffuser followers.

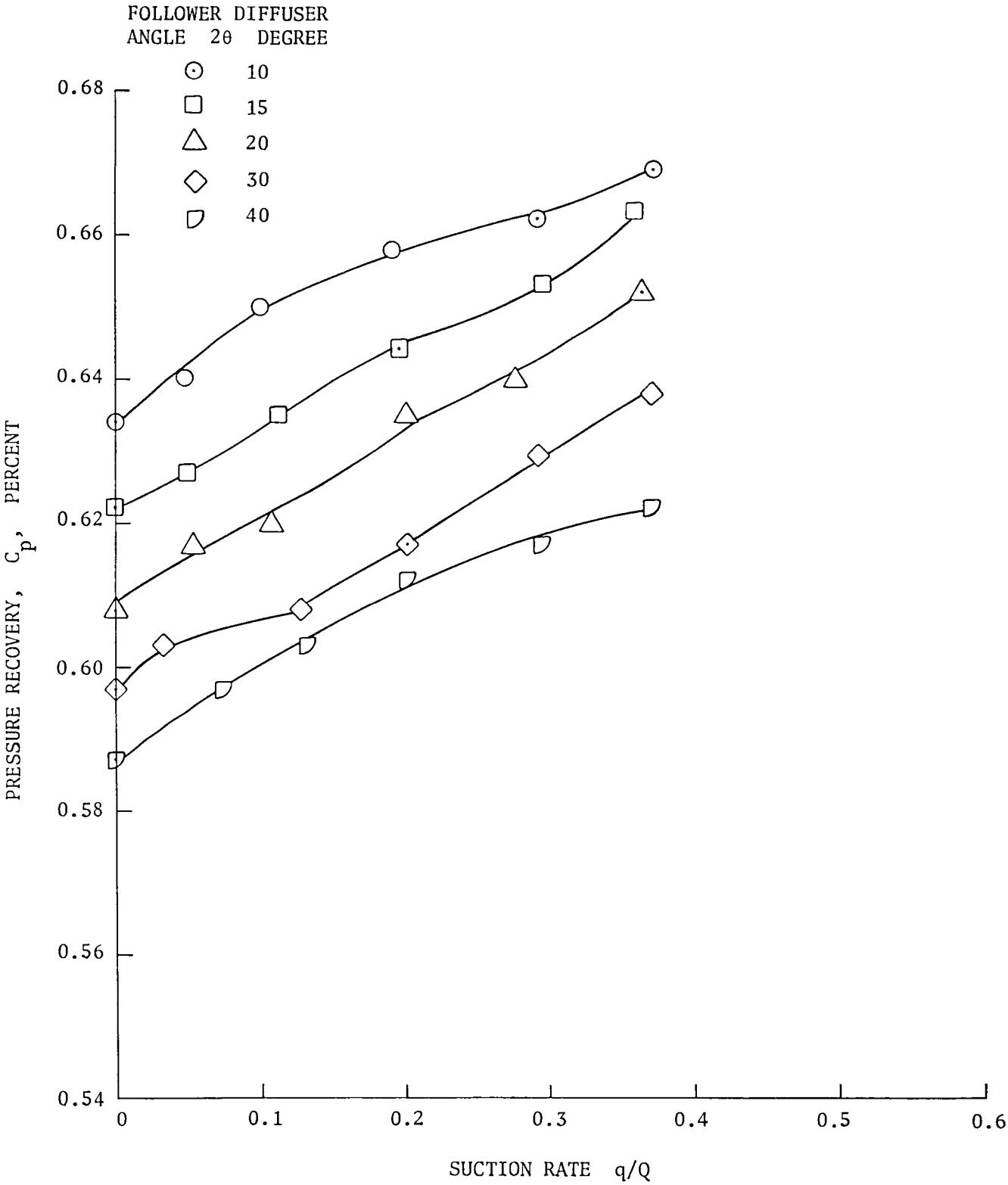

(b) Reynolds number $R_e = 2.87 \times 10^5$.

Figure 5. (Continued)

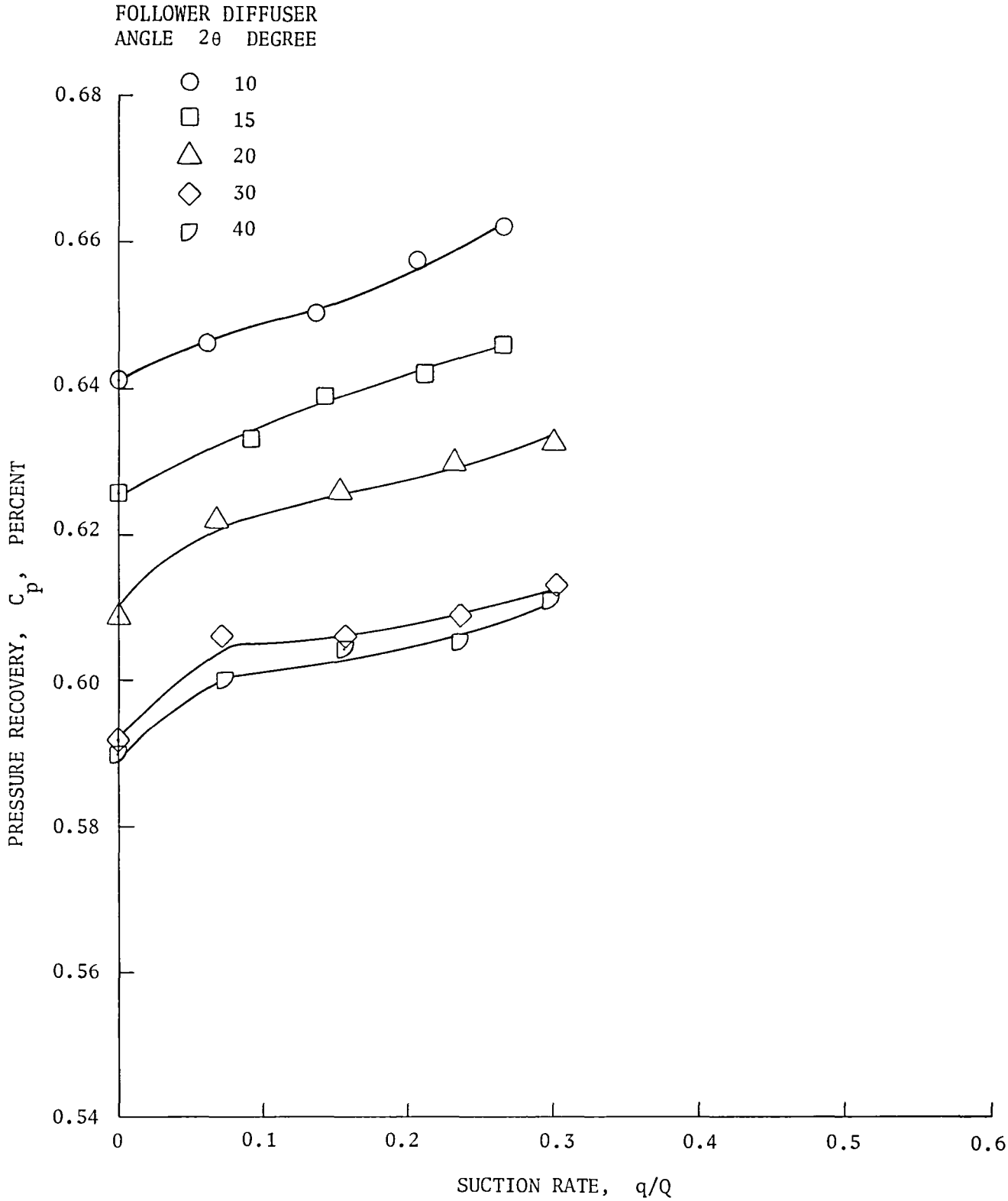

(c) Reynolds number $R_e = 4 \times 10^5$.

Figure 5. (Continued)

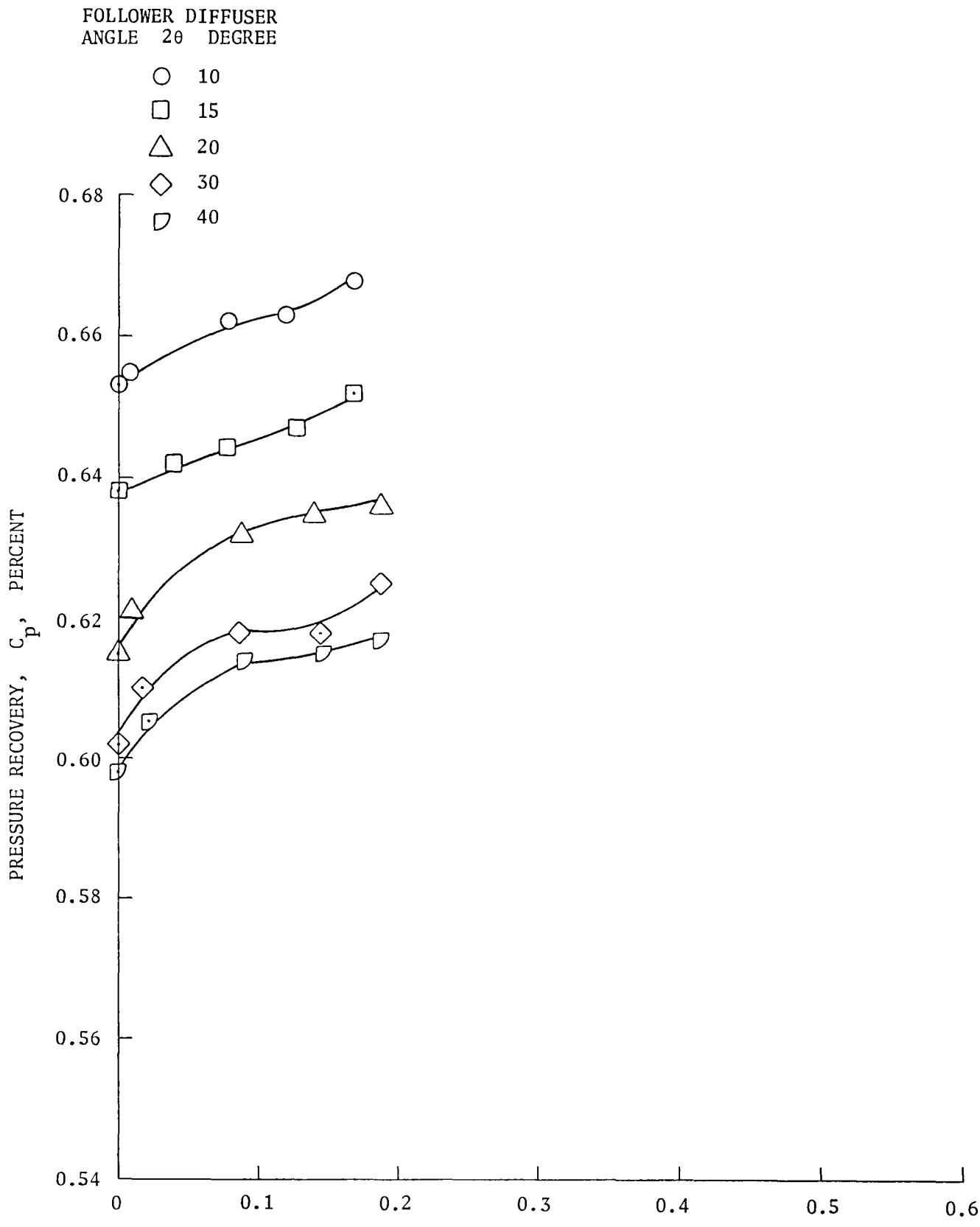

(d) Reynolds number $R_e = 6.12 \times 10^5$.

Figure 5. (Continued)

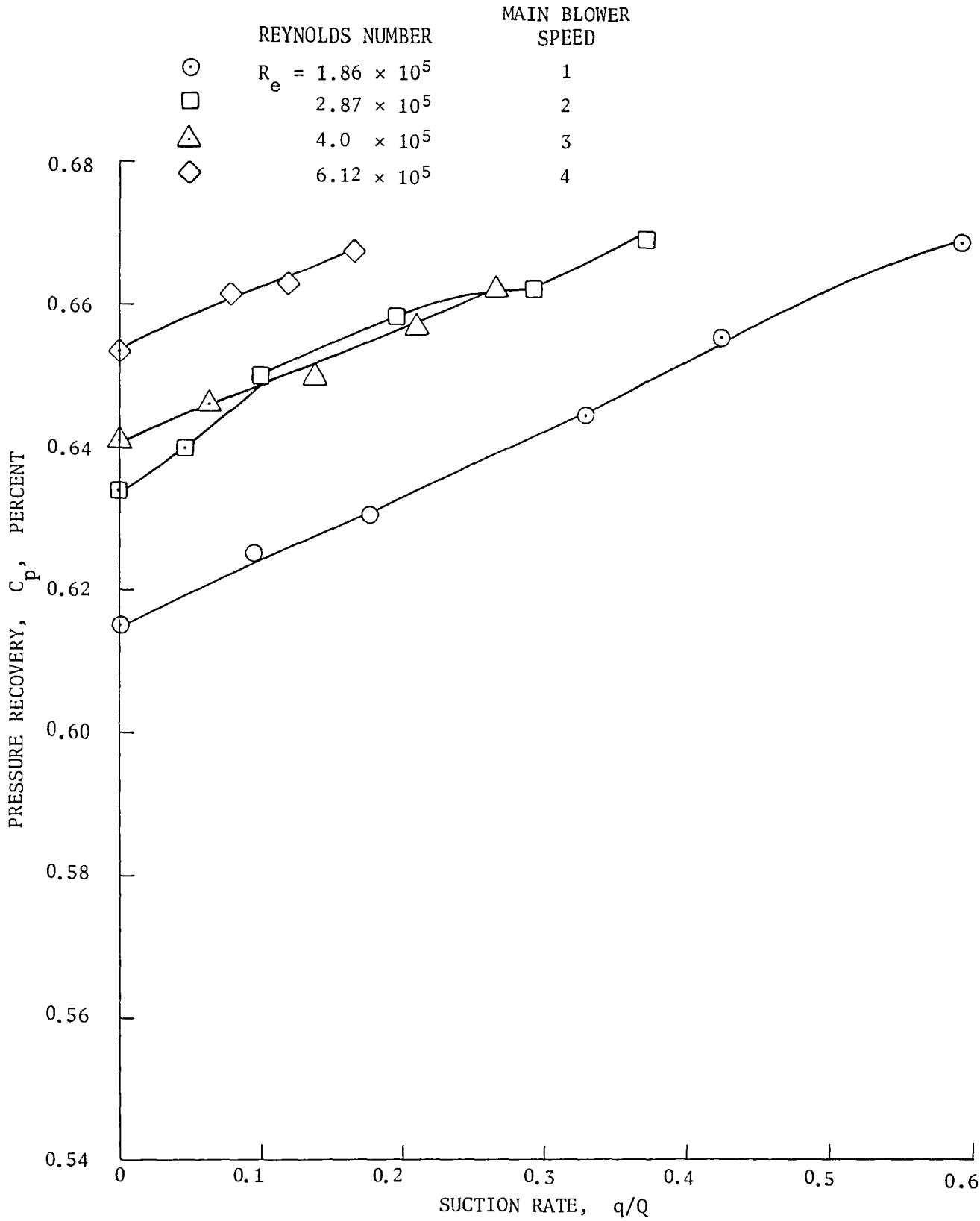

(a) Follower angle $2\theta = 10°$.

Figure 6. Effects of suction on pressure recovery at different Reynolds numbers for the same diffuser.

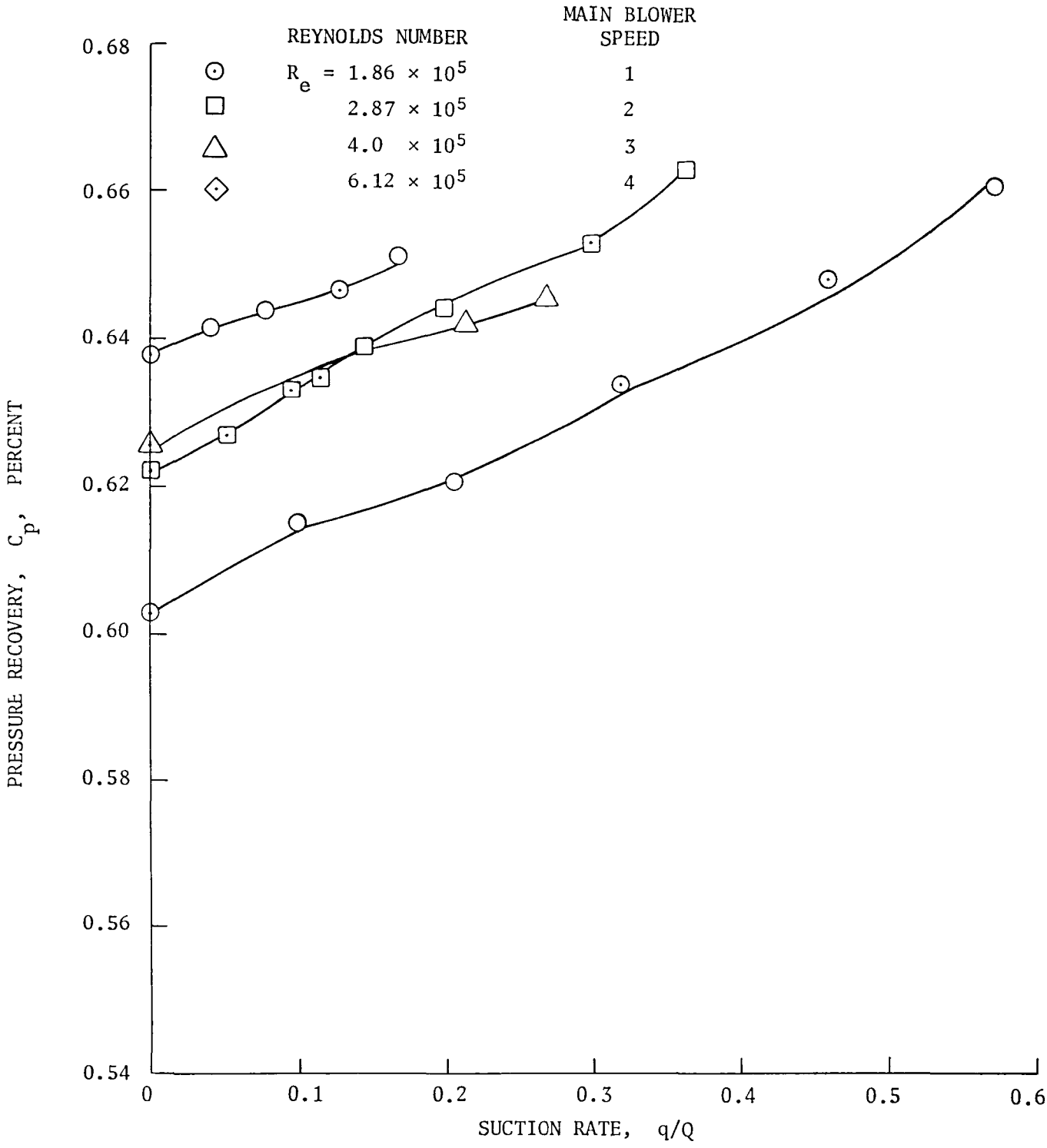

(b) Follower angle $2\theta = 15°$.

Figure 6. (Continued)

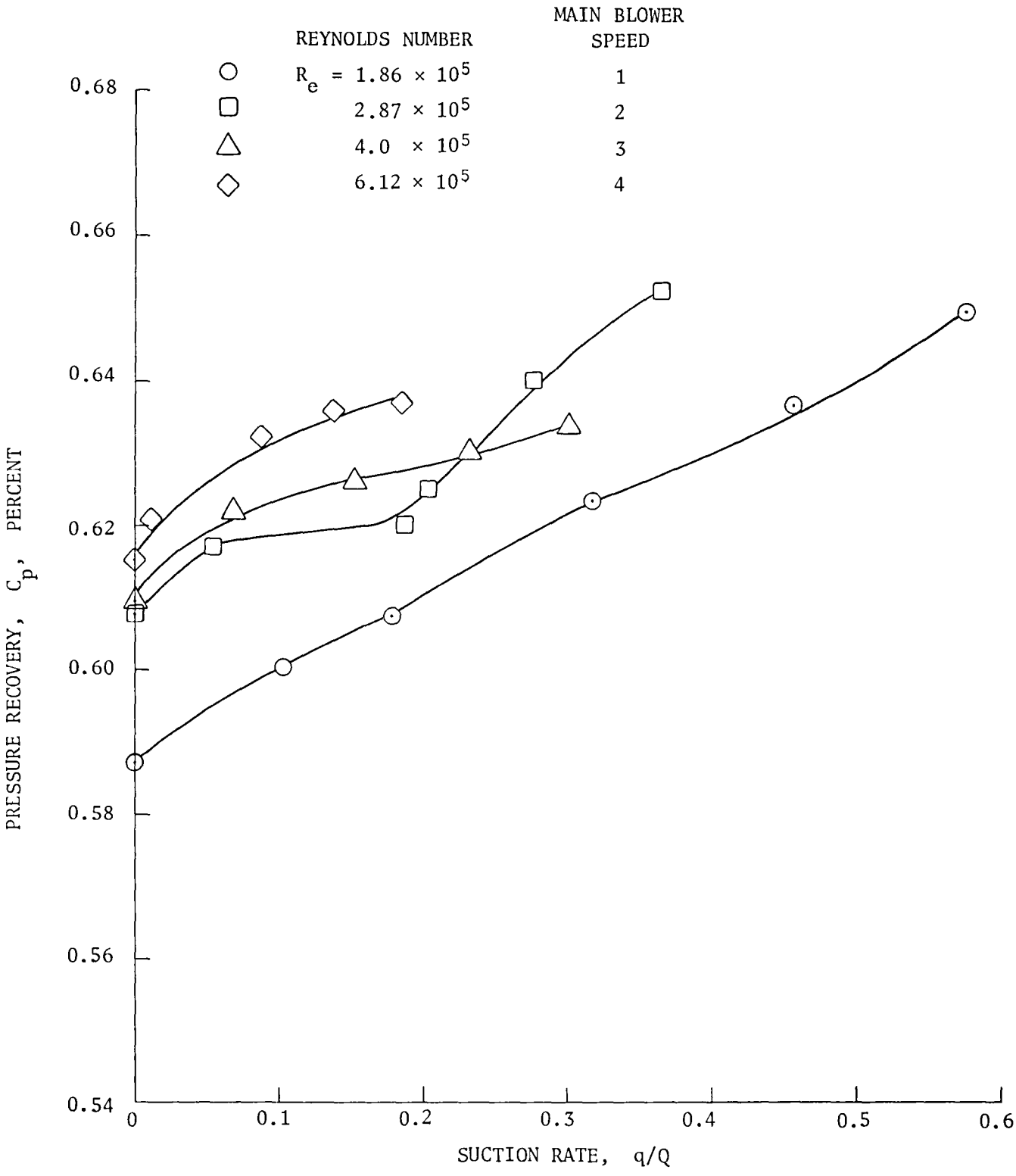

(c) Follower angle $2\theta = 20°$.

Figure 6. (Continued)

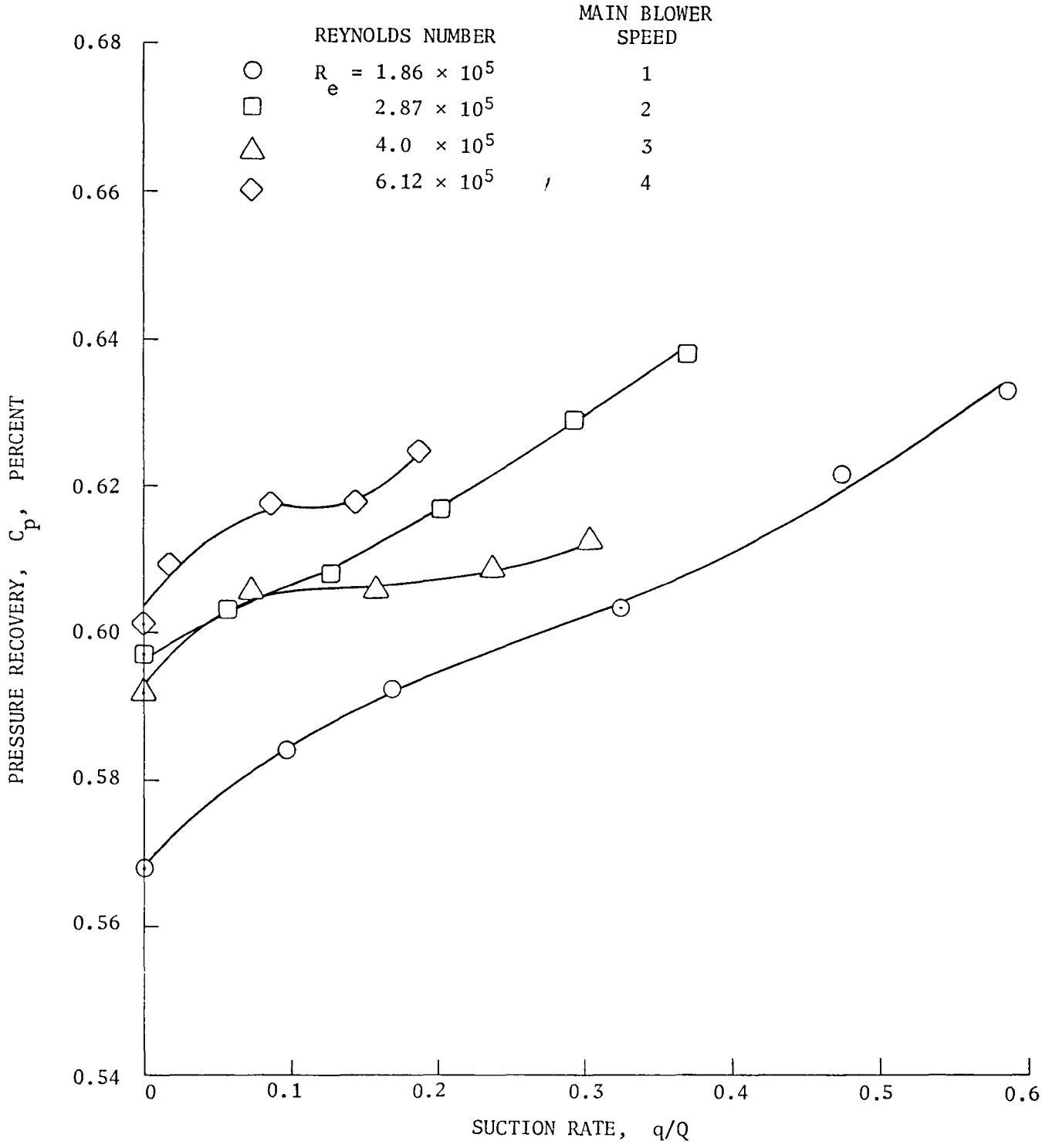

(d) Follower angle $2\theta = 30°$.

Figure 6. (Continued)

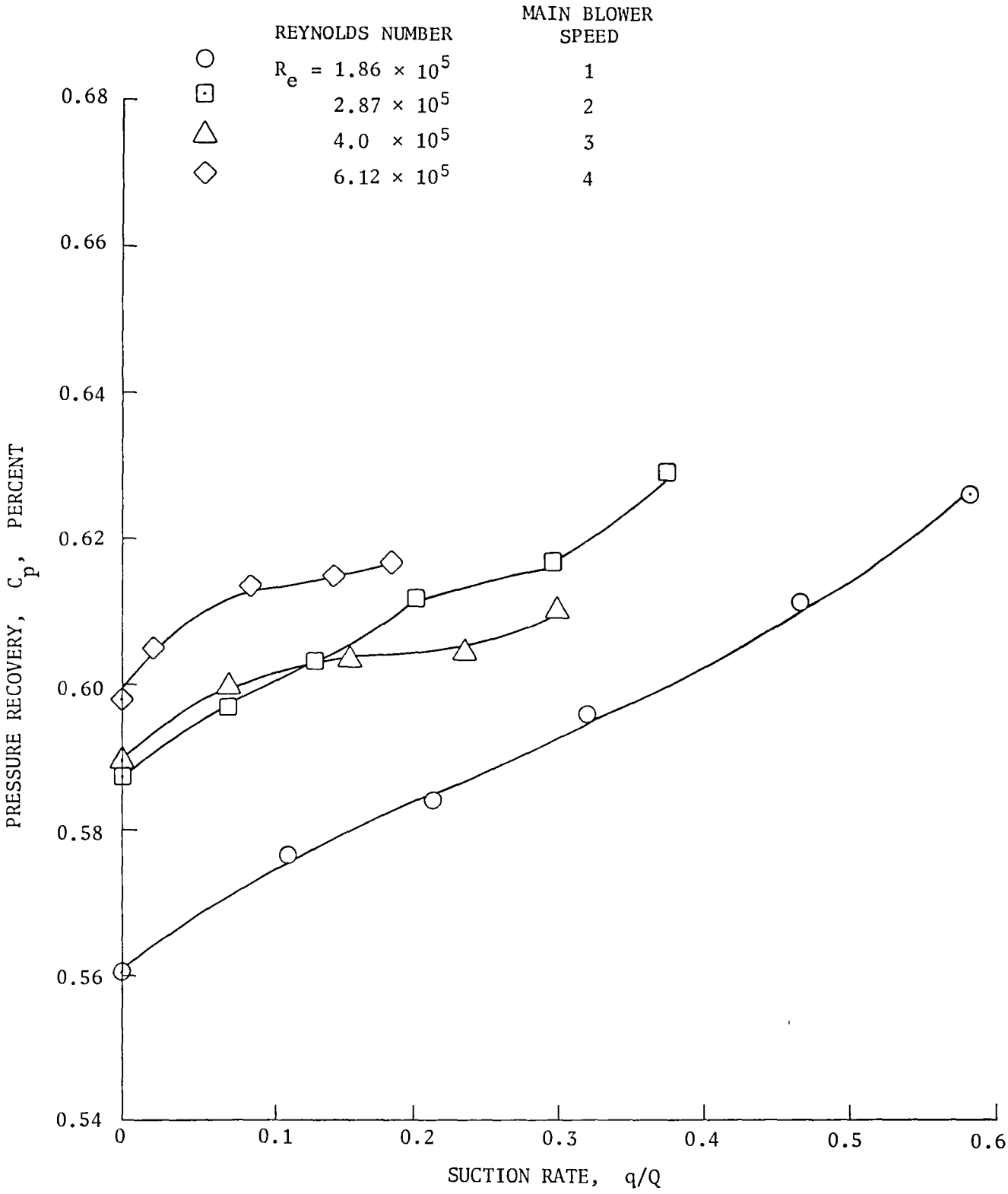

(e) Follower angle $2\theta = 40°$.

Figure 6. (Concluded)

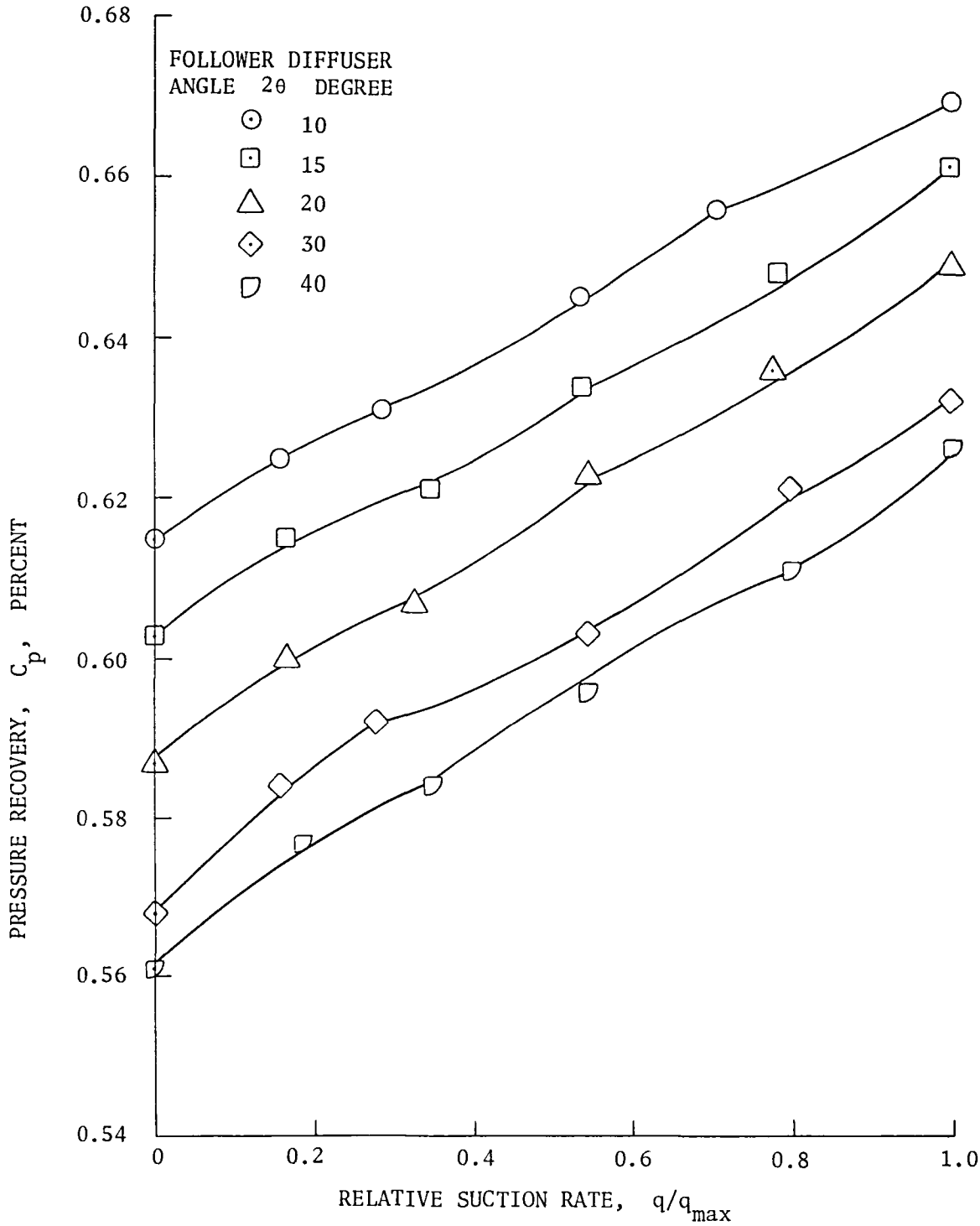

(a) Reynolds number $R_e = 1.86 \times 10^5$.

Figure 7. Effects of suction on pressure recovery at constant Reynolds numbers for various diffuser followers.

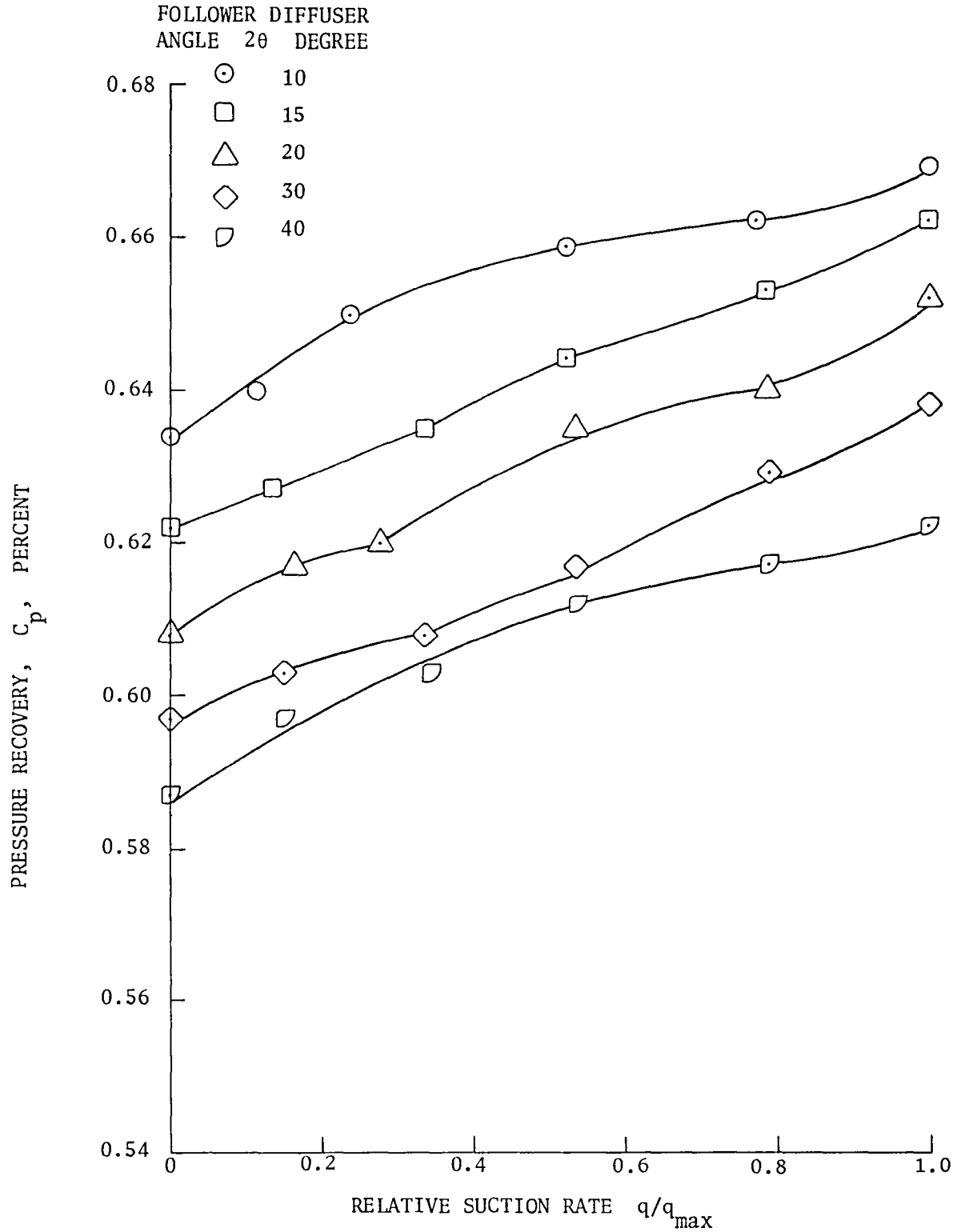

(b) Reynolds number $R_e = 2.87 \times 10^5$.

Figure 7. (Continued)

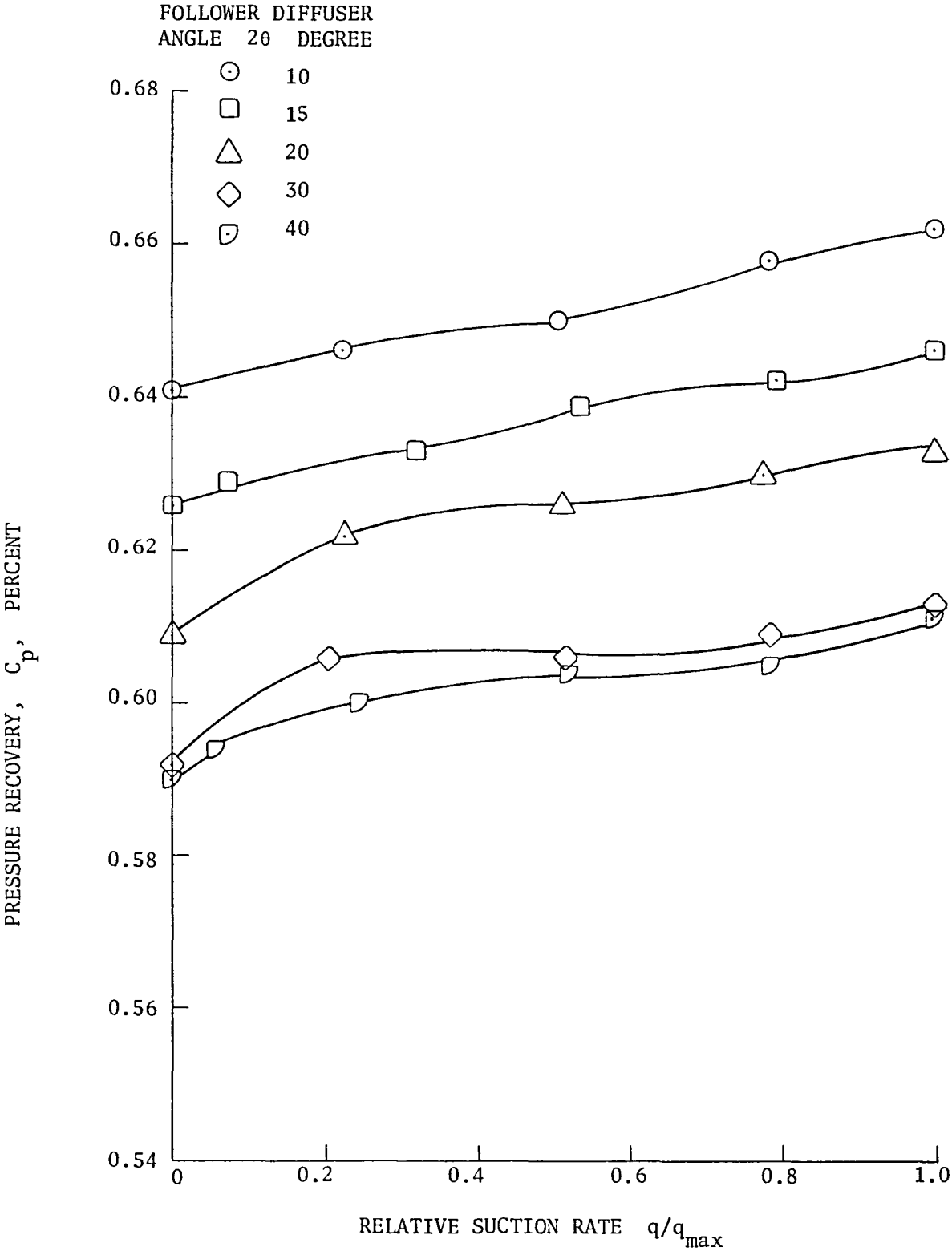

(c) Reynolds number $R_e = 4 \times 10^5$.

Figure 7. (Continued)

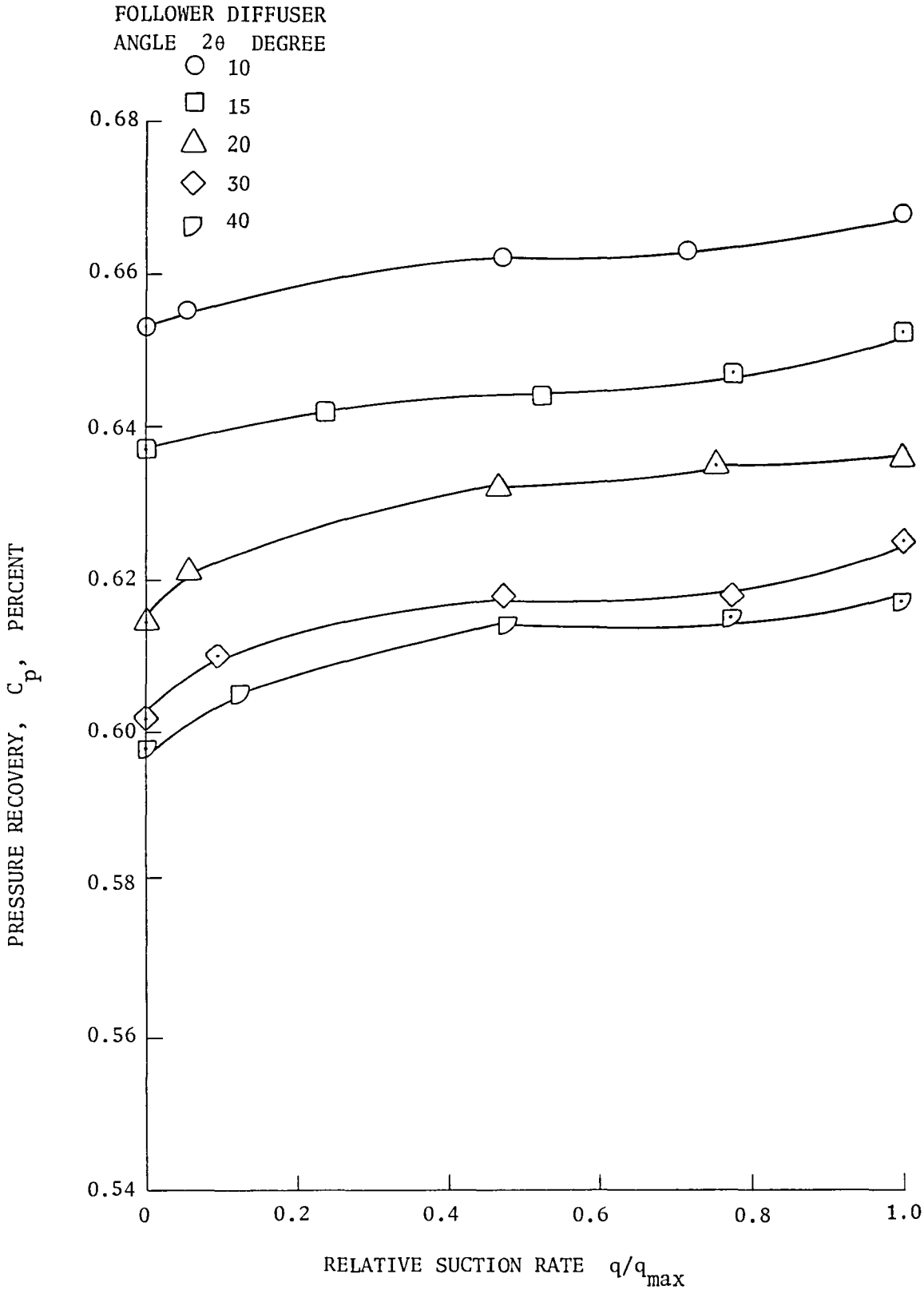

(d) Reynolds number $R_e = 6.12 \times 10^5$.

Figure 7. (Concluded)

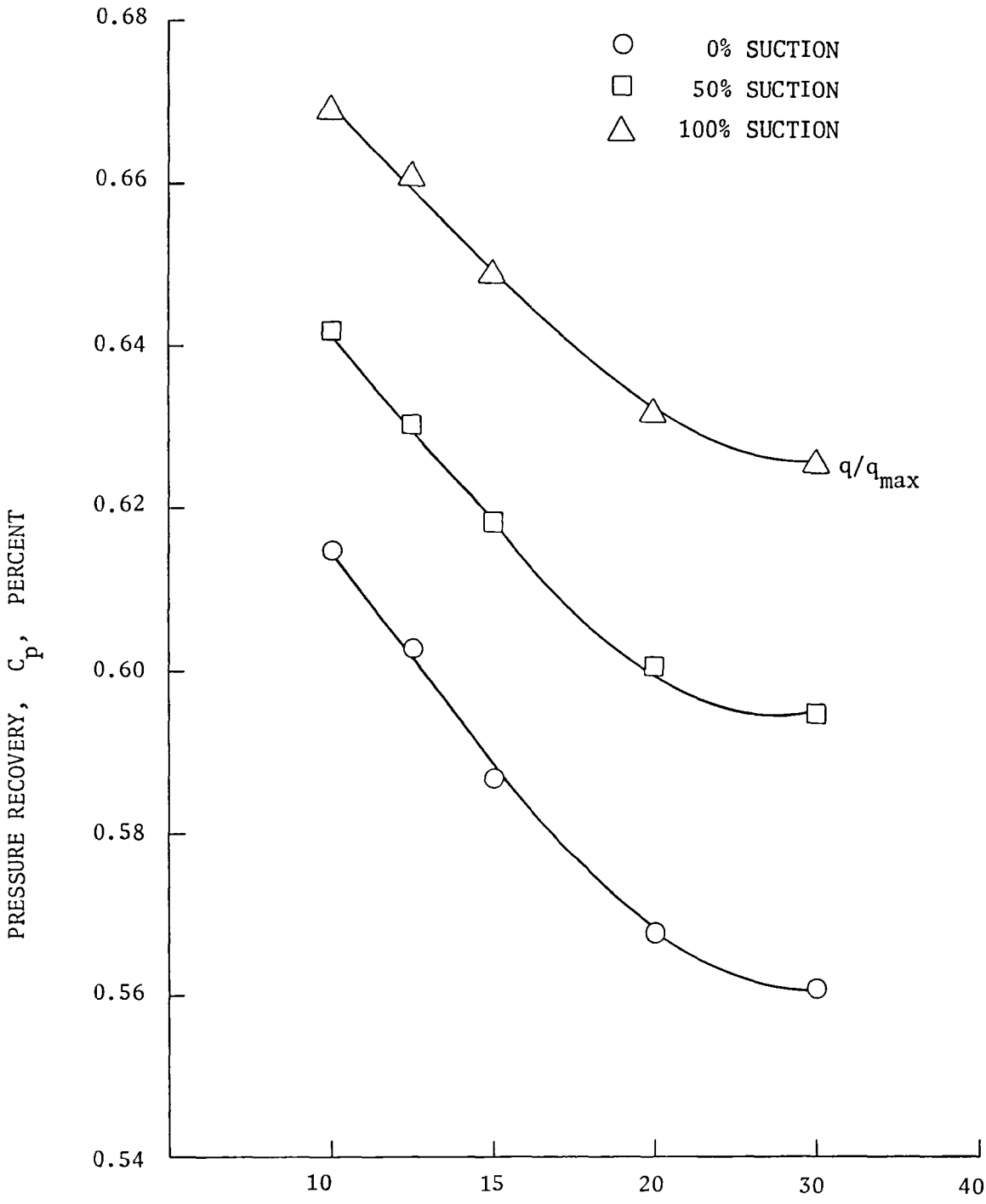

(a) Reynolds number $R_e = 1.86 \times 10^5$.

Figure 8. Variation of pressure recovery with follower diffuser angle for three suction rates at specified Reynolds numbers.

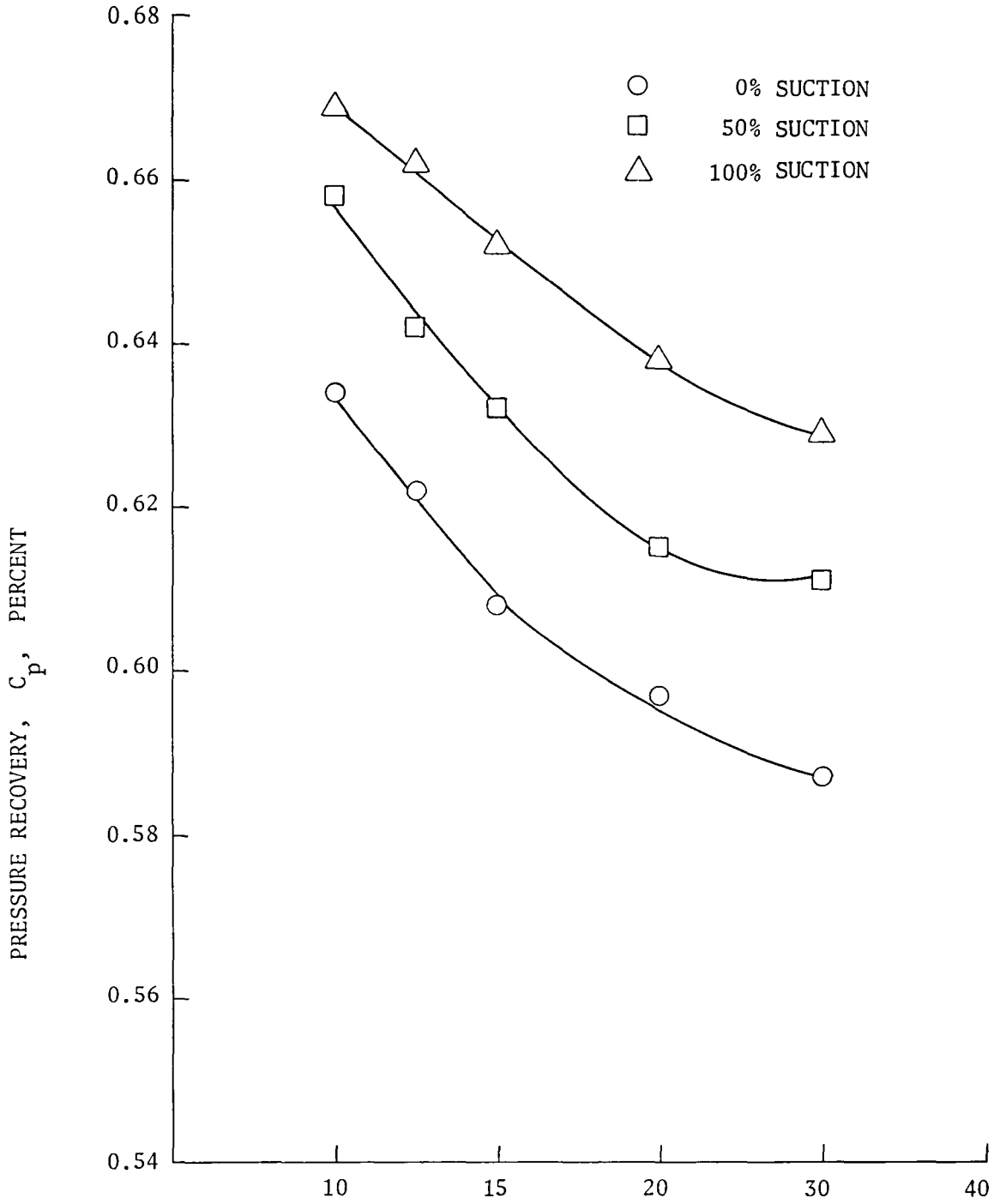

(b) Reynolds number $R_e = 2.87 \times 10^5$.

Figure 8. (Continued)

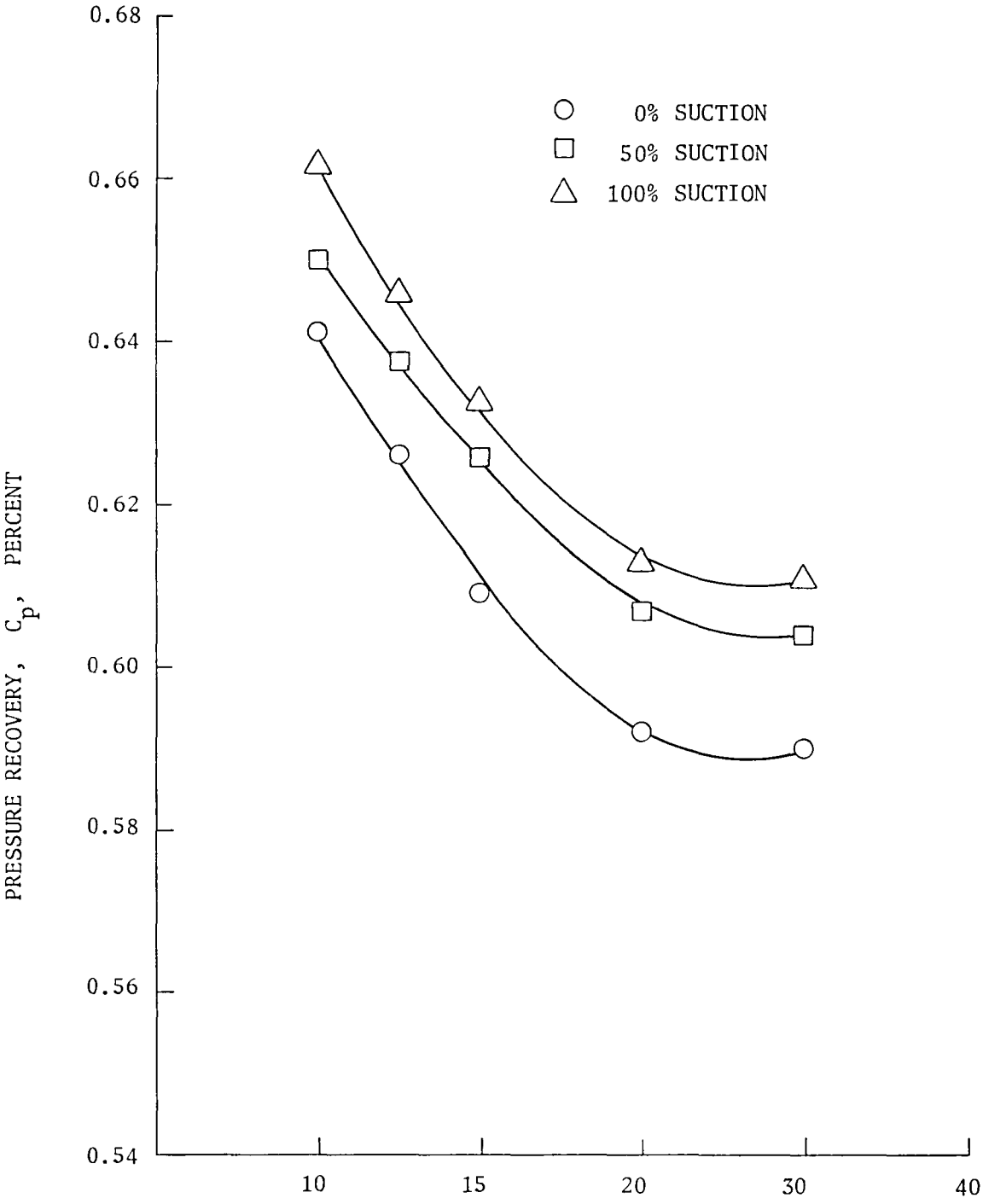

(c) Reynolds number $R_e = 4 \times 10^5$.

Figure 8. (Concluded)

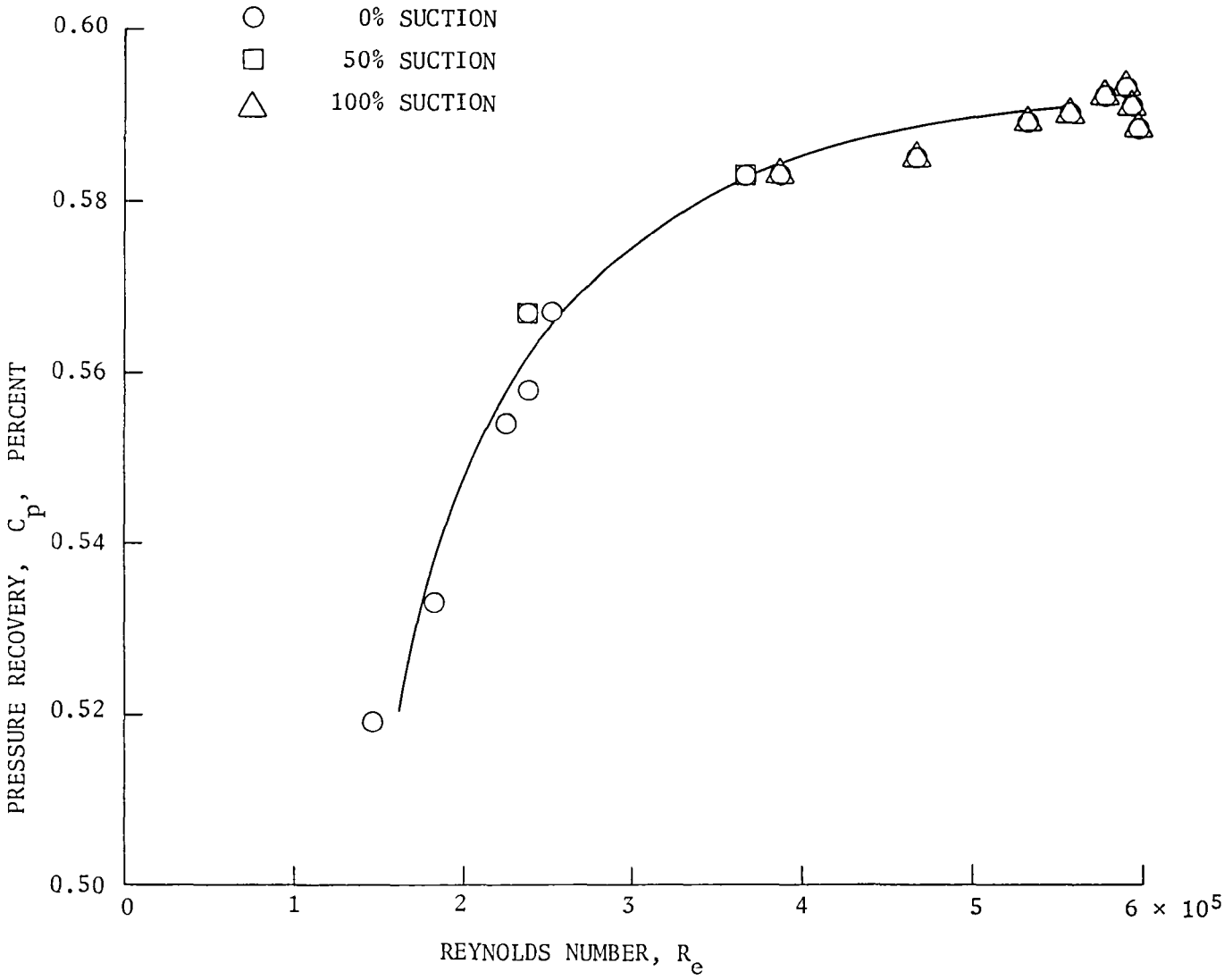

Figure 9. Variation of pressure recovery with Reynolds number in leading diffuser ($2\theta = 4.8°$).

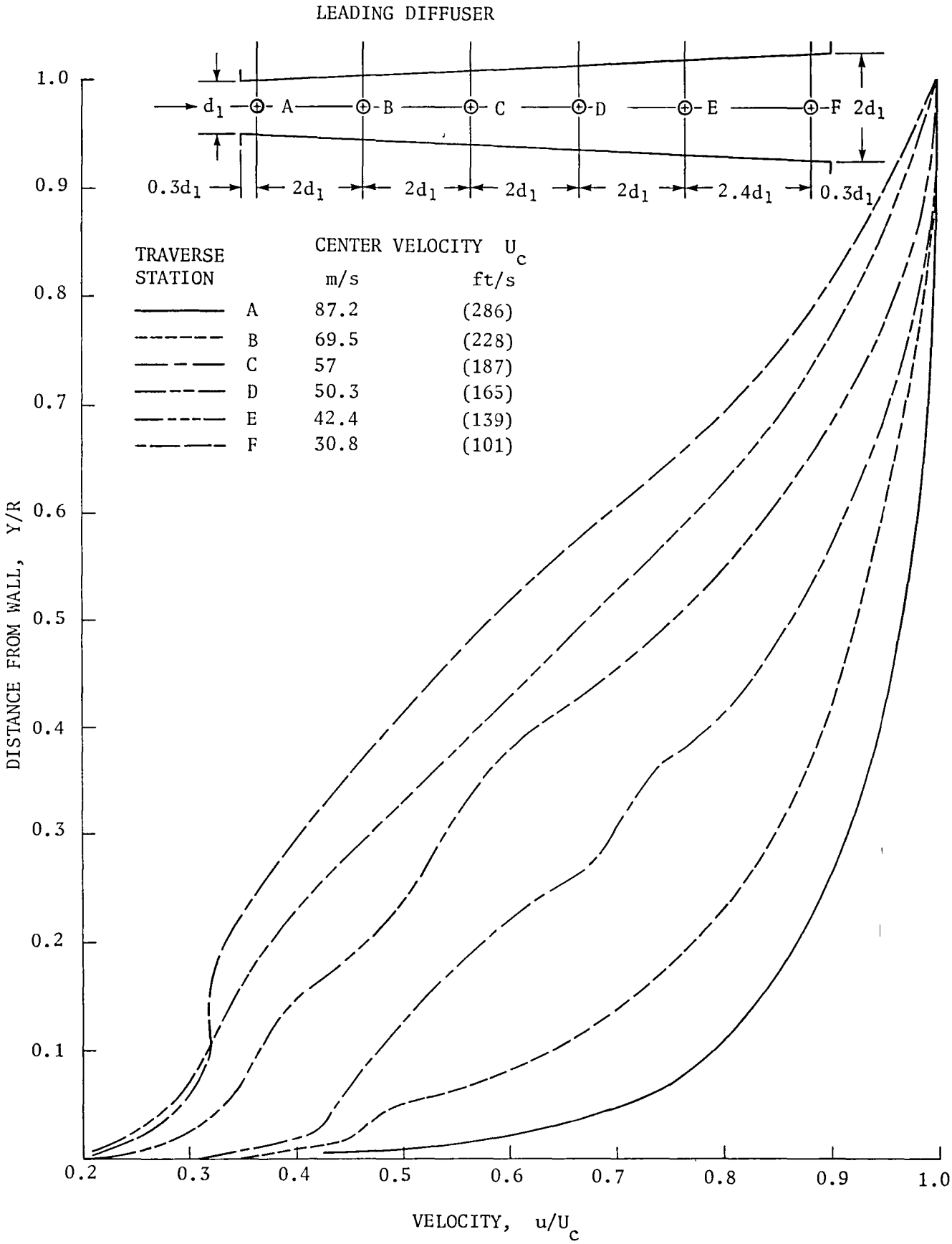

Figure 10. Velocity distributions along leading diffuser at Reynolds number R_e = 6.12×10^5. (Traverse stations A to F are shown at top.)

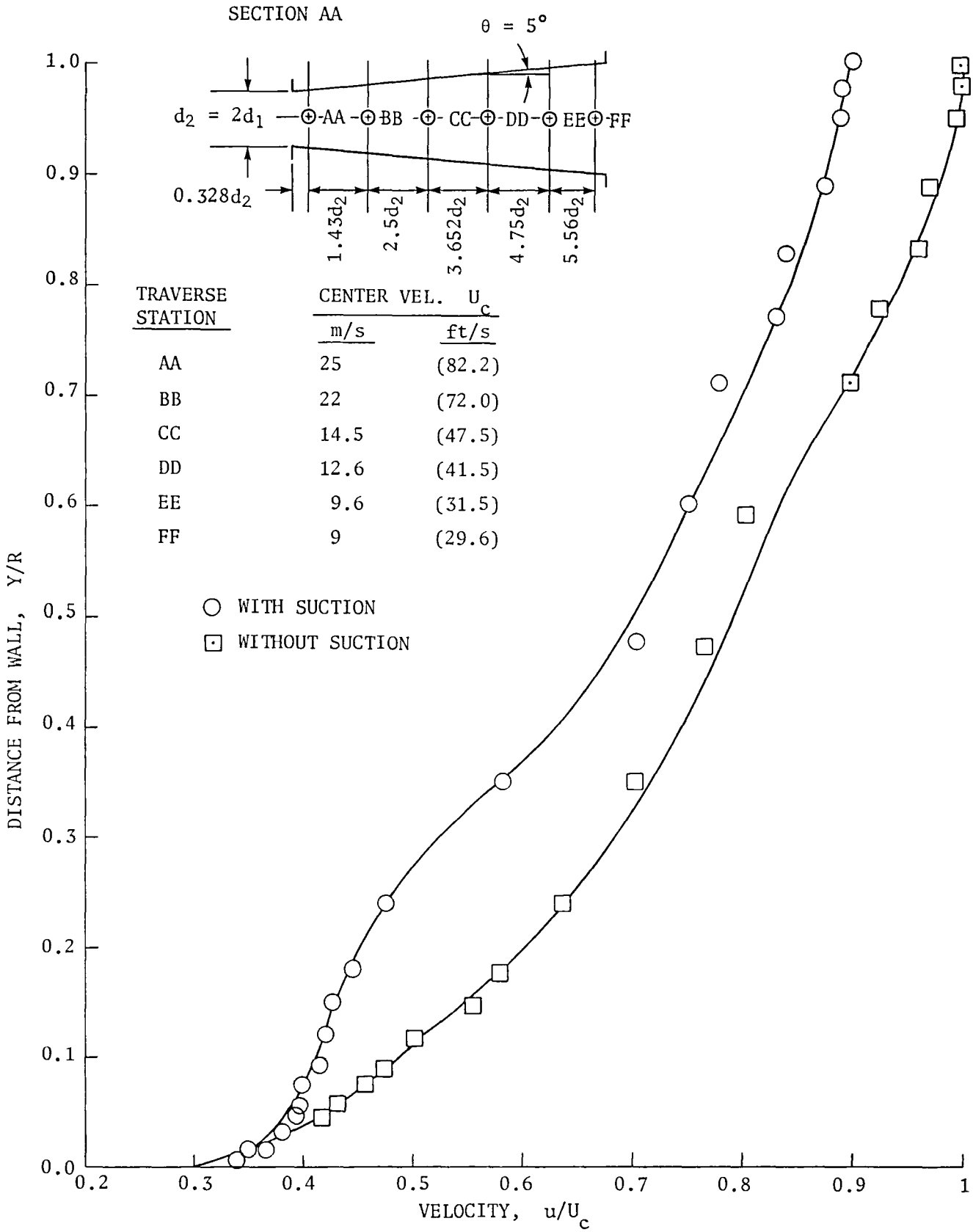

(a) Traverse across section AA.

Figure 11. Velocity distributions along a follower diffuser with $2\theta = 10°$ at Reynolds number $R_e = 4 \times 10^5$ with and without boundary-layer suction.

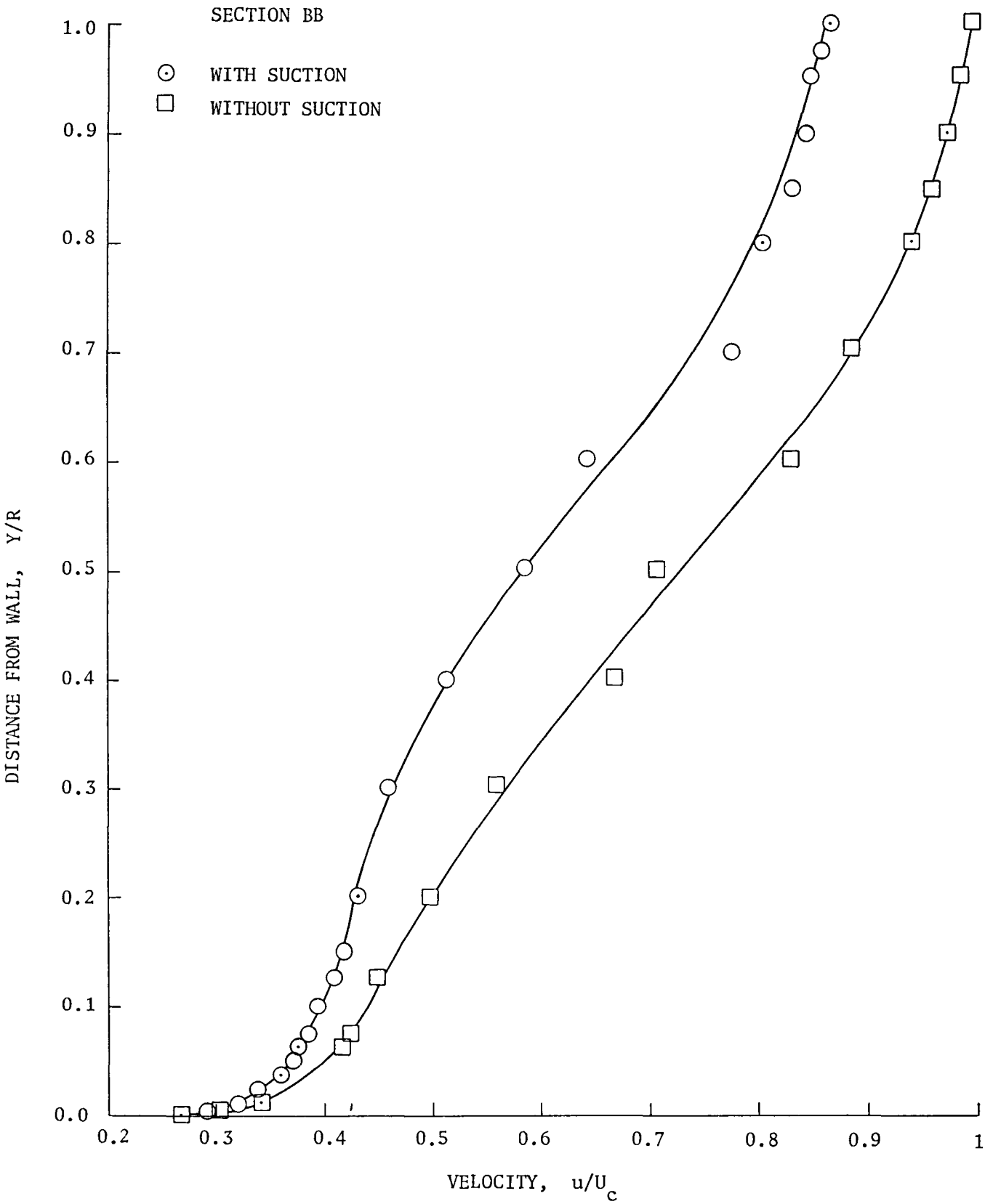

(b) Traverse section BB.

Figure 11. (Continued)

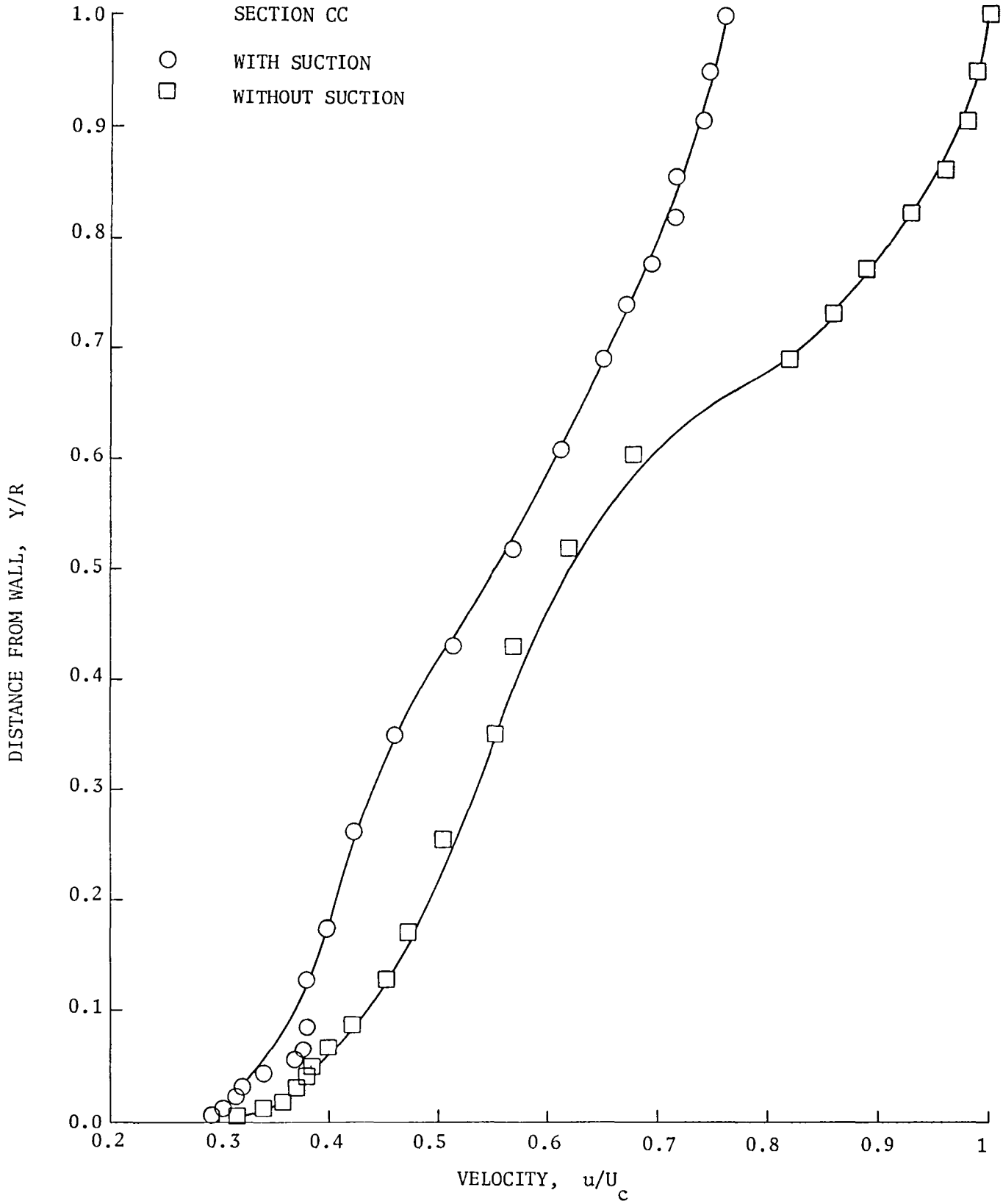

(c) Traverse section CC.
Figure 11. (Continued)

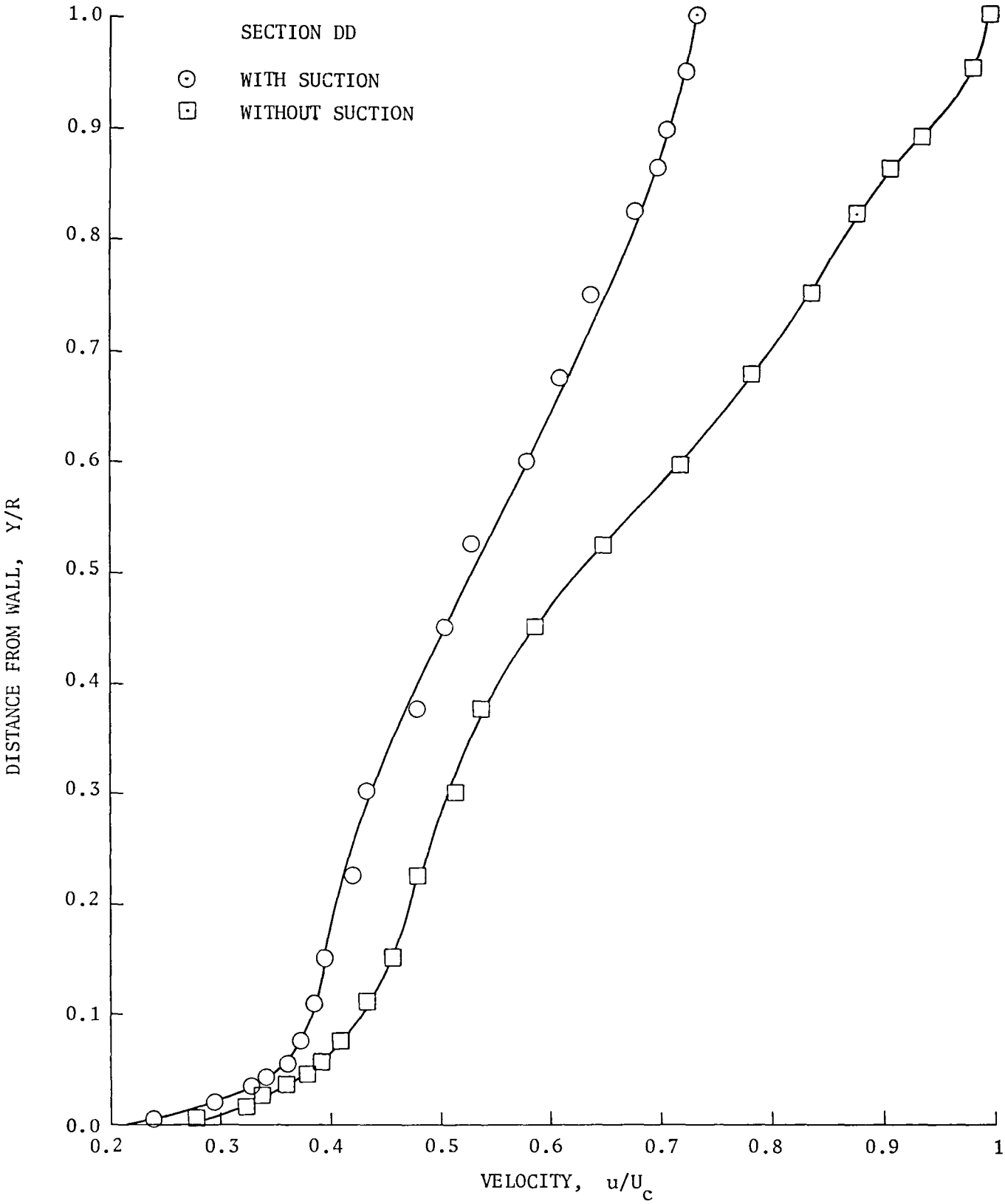

(d) Traverse section DD.

Figure 11. (Continued)

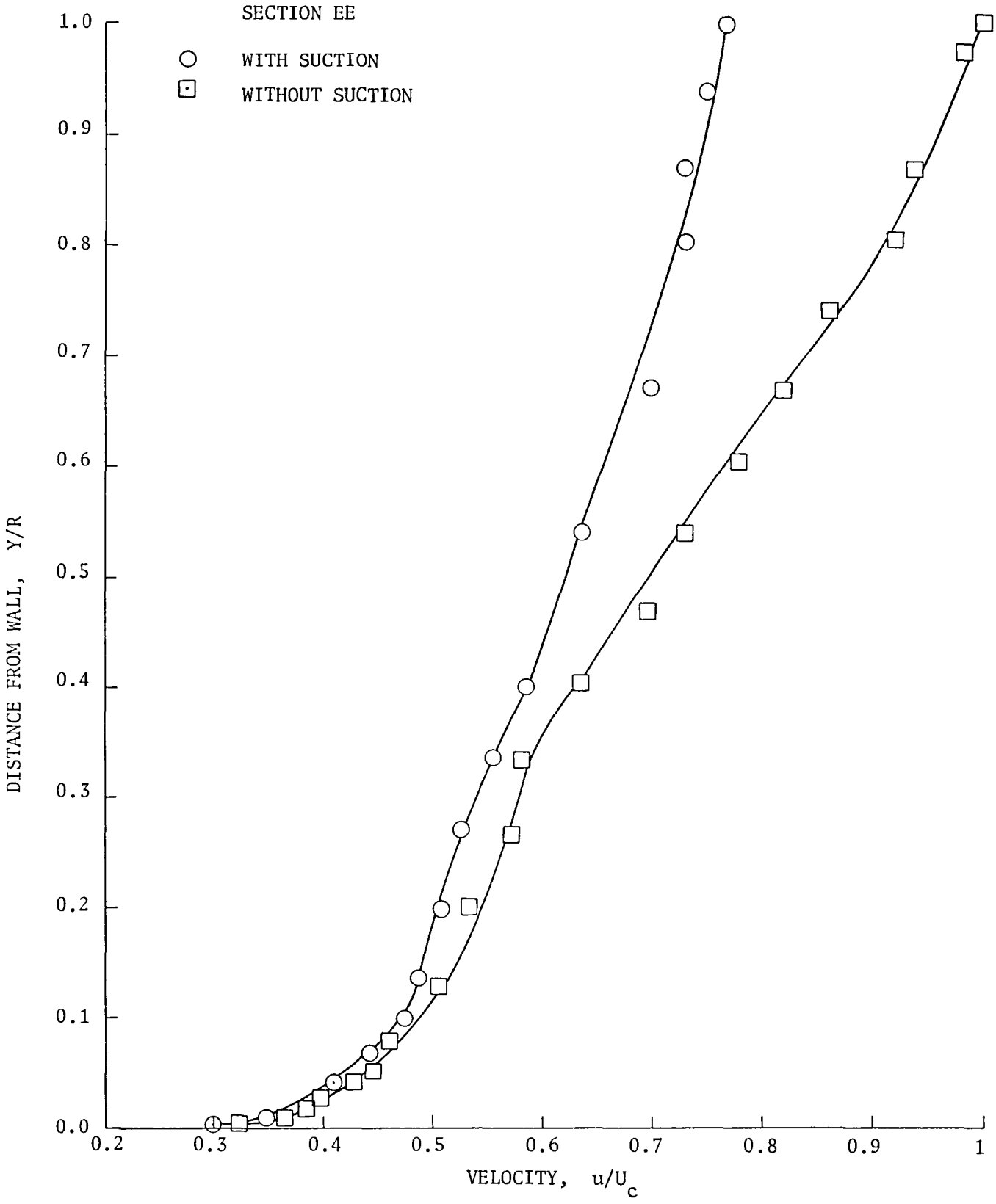

(e) Traverse section EE.

Figure 11. (Continued)

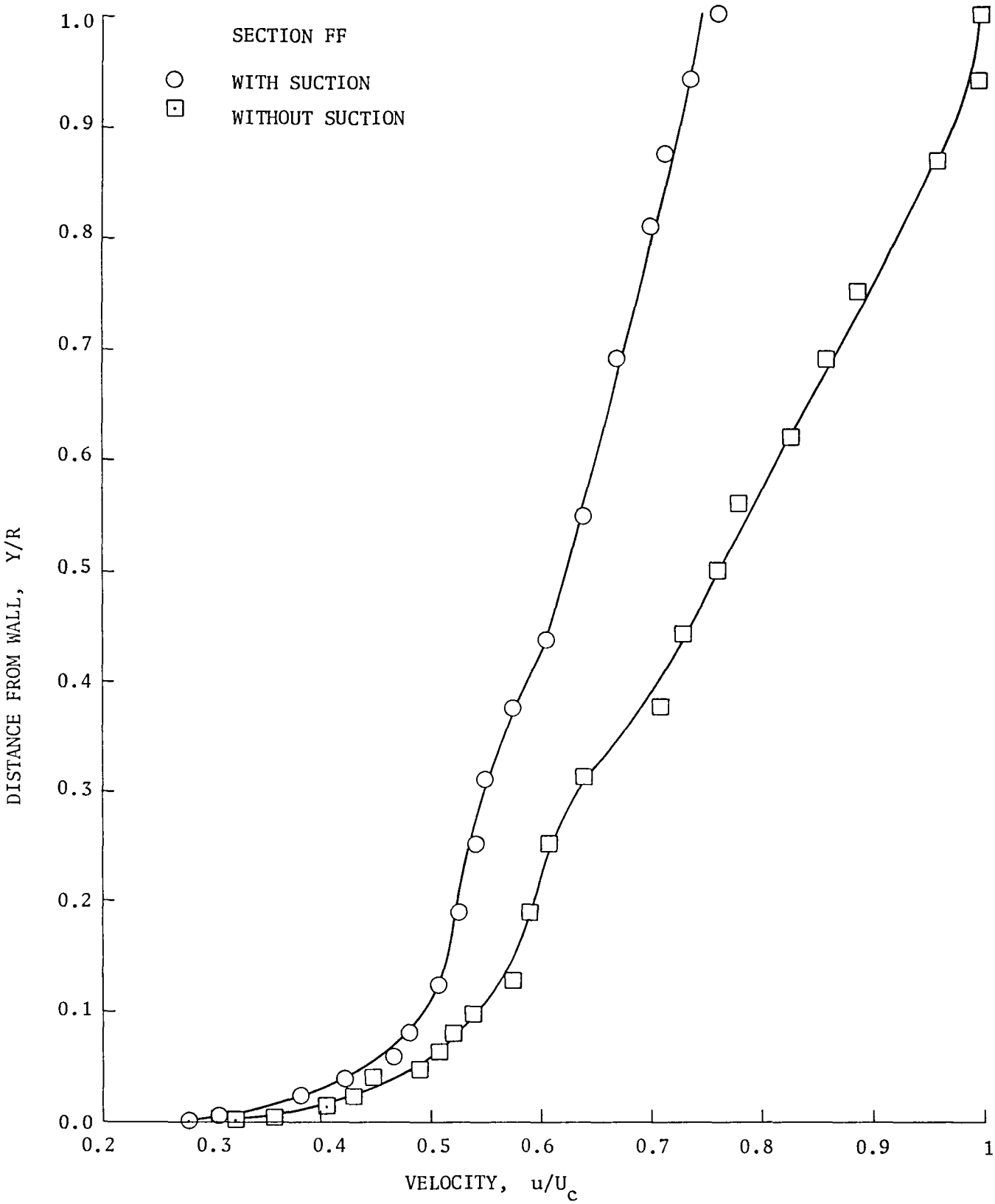

(f) Traverse section FF.

Figure 11. (Concluded)

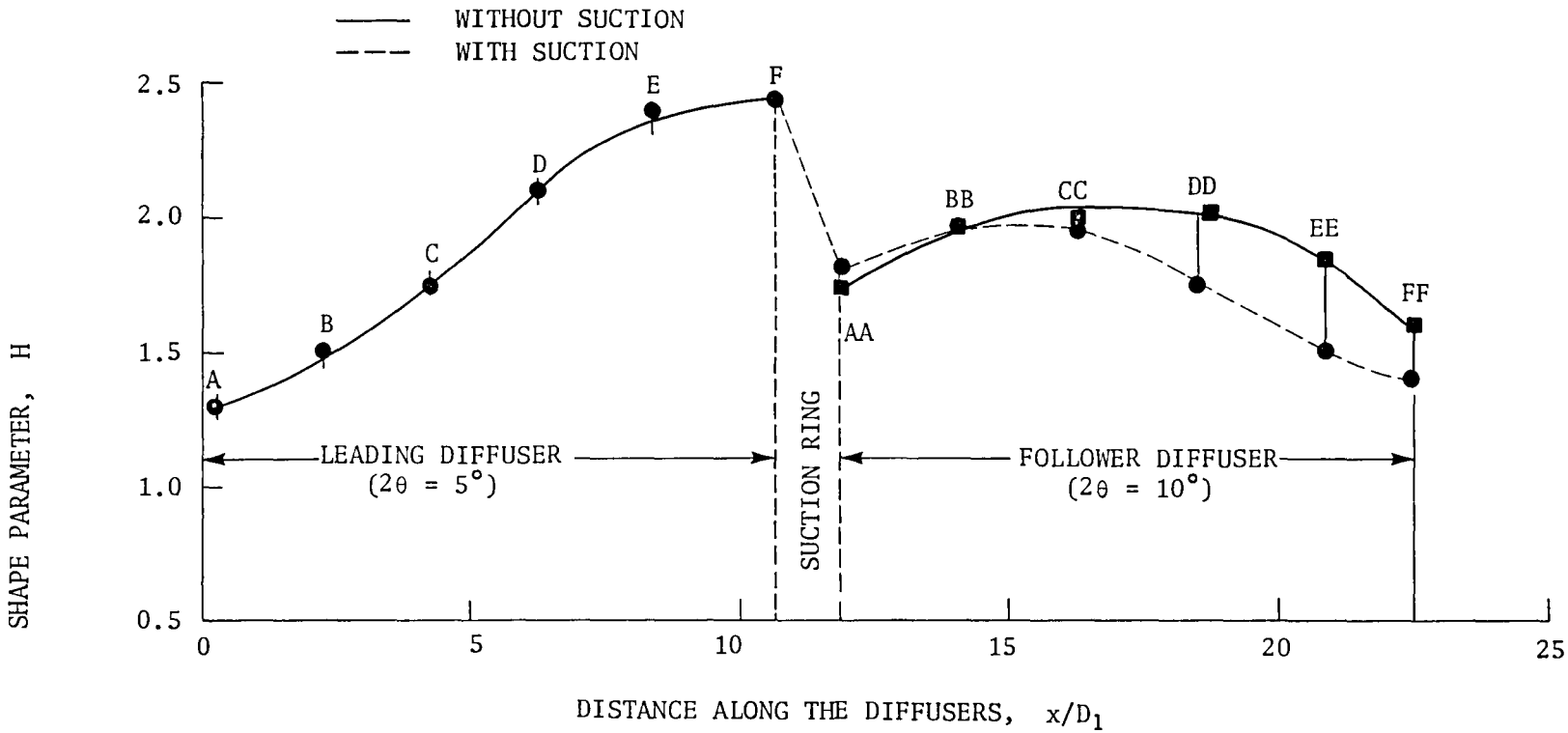

Figure 12. Variation of the shape parameter H along the flow at Reynolds Number $R_e = 6.12 \times 10^5$ with and without suction.

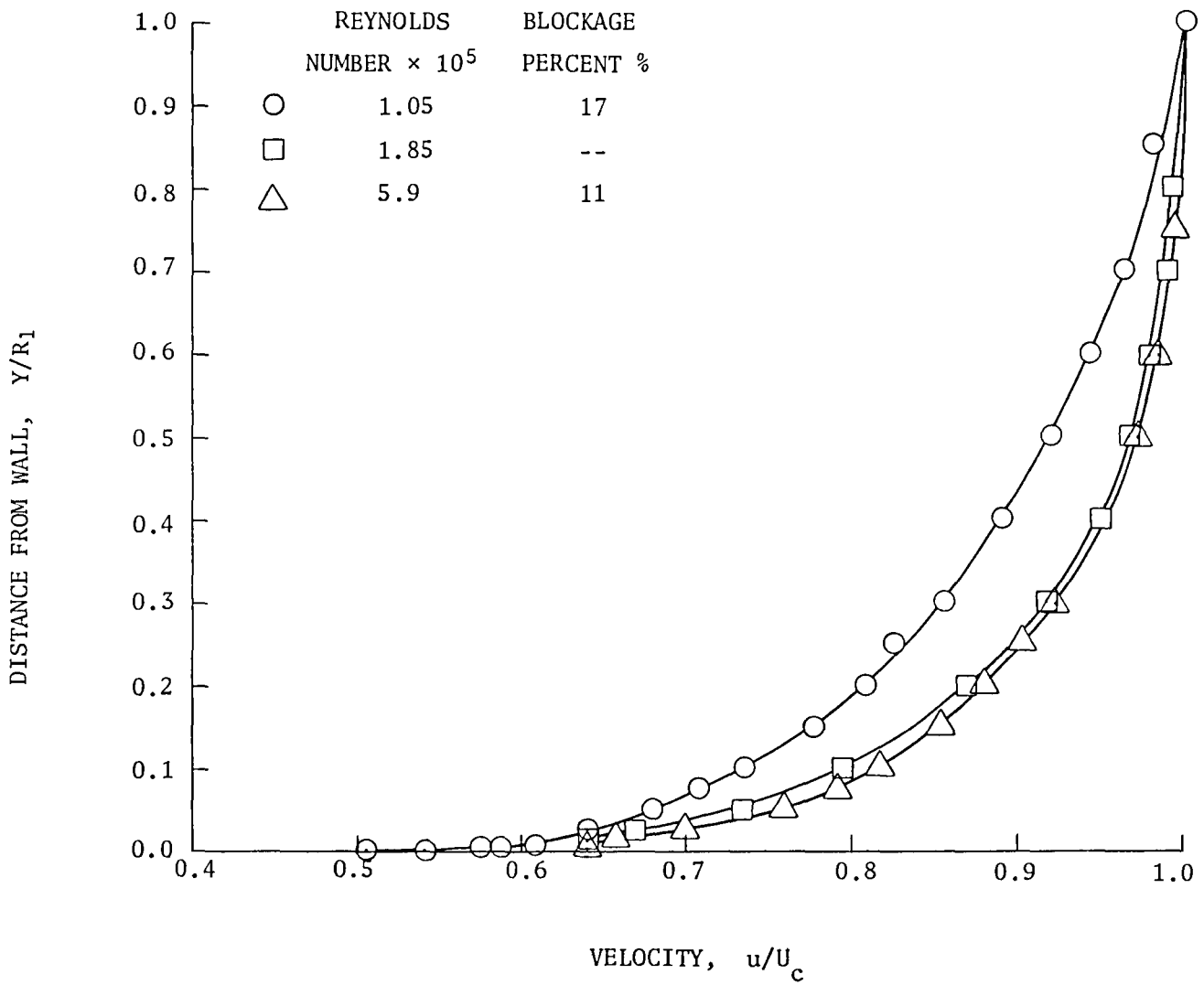

Figure 13. Velocity distribution in the T_1 plane for three different Reynolds numbers.

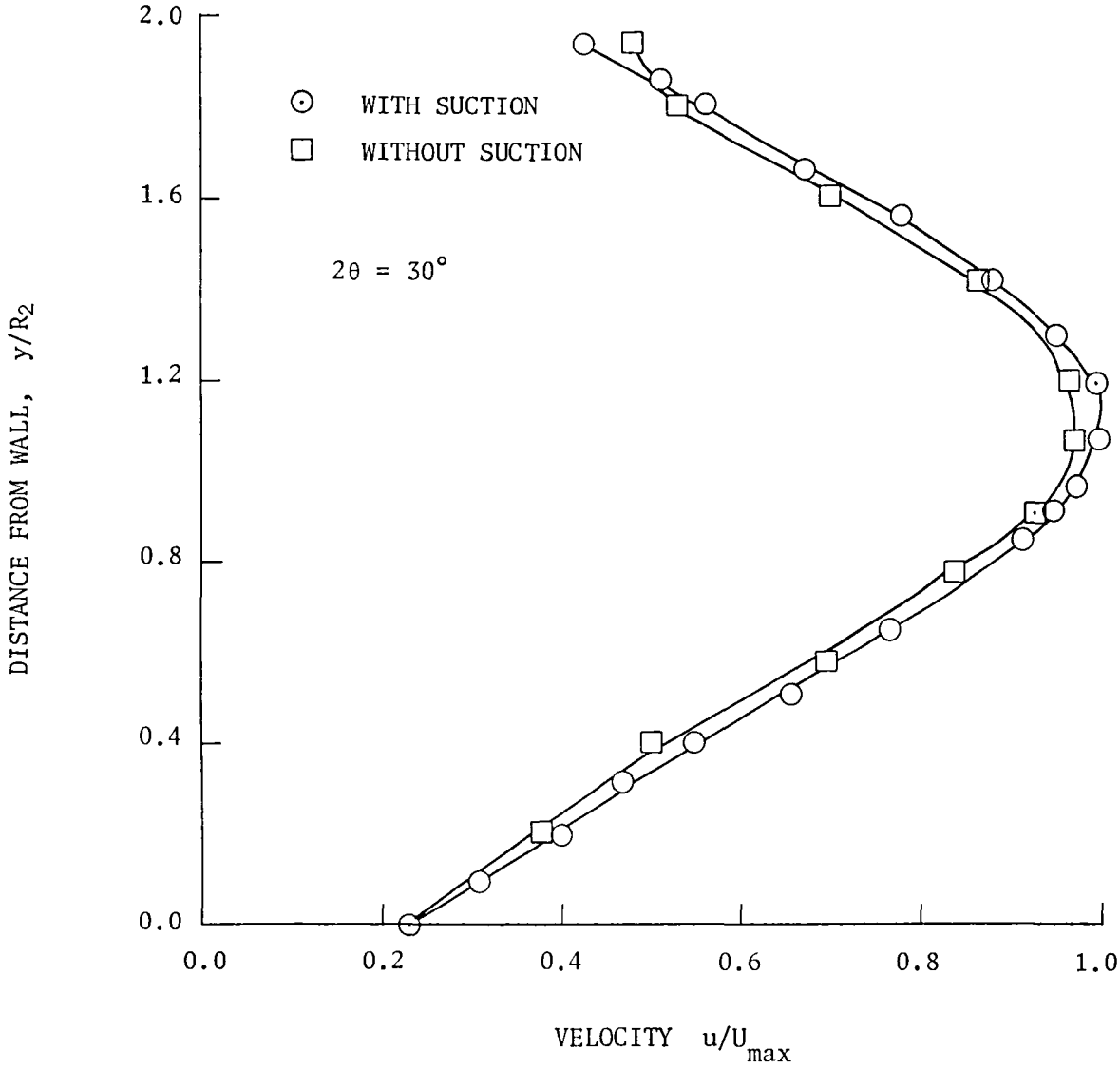

Figure 14. Velocity distribution with or without suction in the T_2 plane upstream from the suction ring; Reynolds number $R_e = 4 \times 10^5$; suction rate $q/Q = 0.288$; maximum velocity $U_{max} = 26$ m/s (85.3 ft/s).

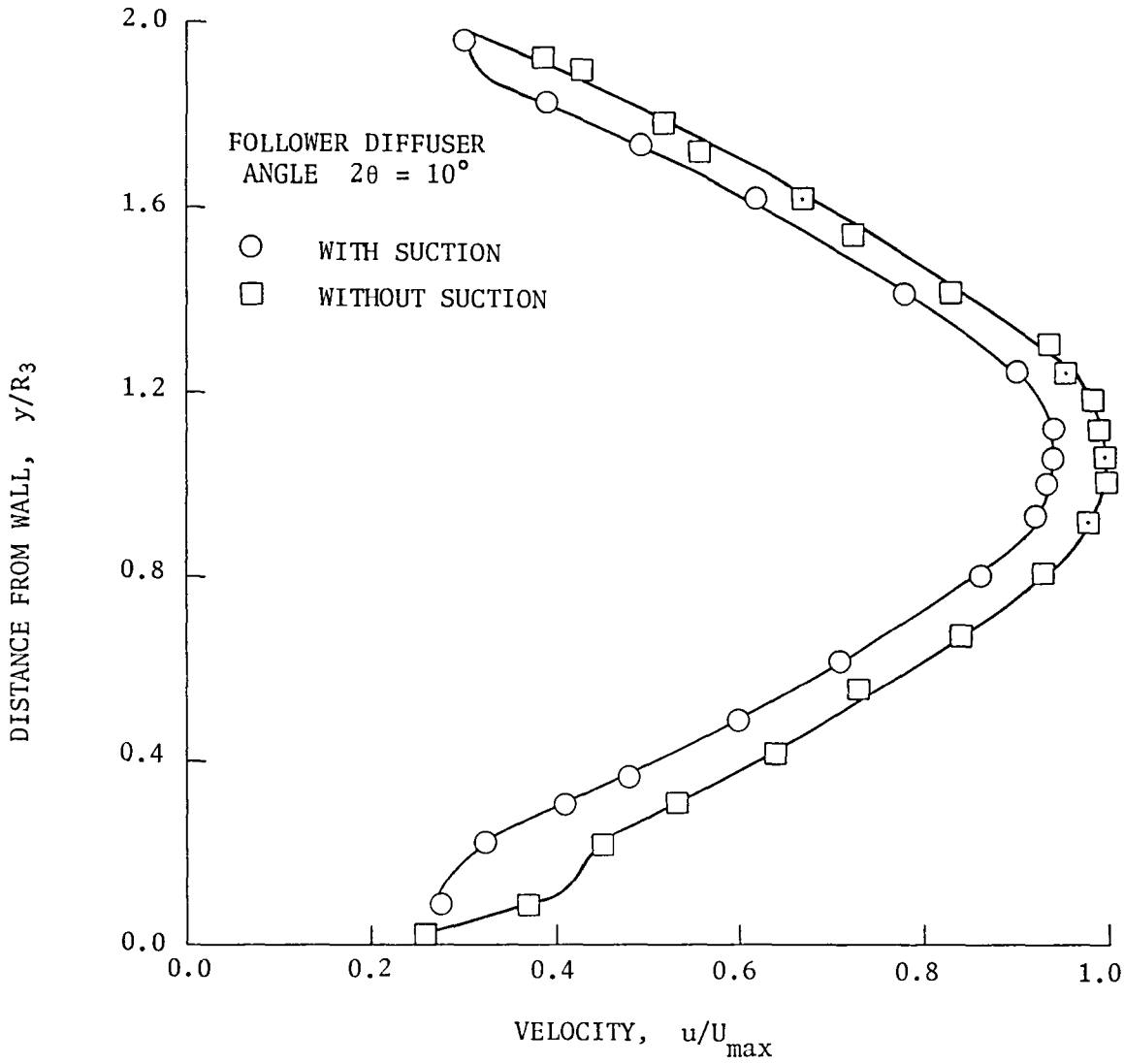

Figure 15. Velocity distribution with or without suction in the T_3 plane immediately downstream from the suction ring; Reynolds number $R_e = 2.87 \times 10^5$, suction rate $q/Q = 0.21$; maximum velocity $U_{max} = 17.7$ m/s (58.1 ft/s).

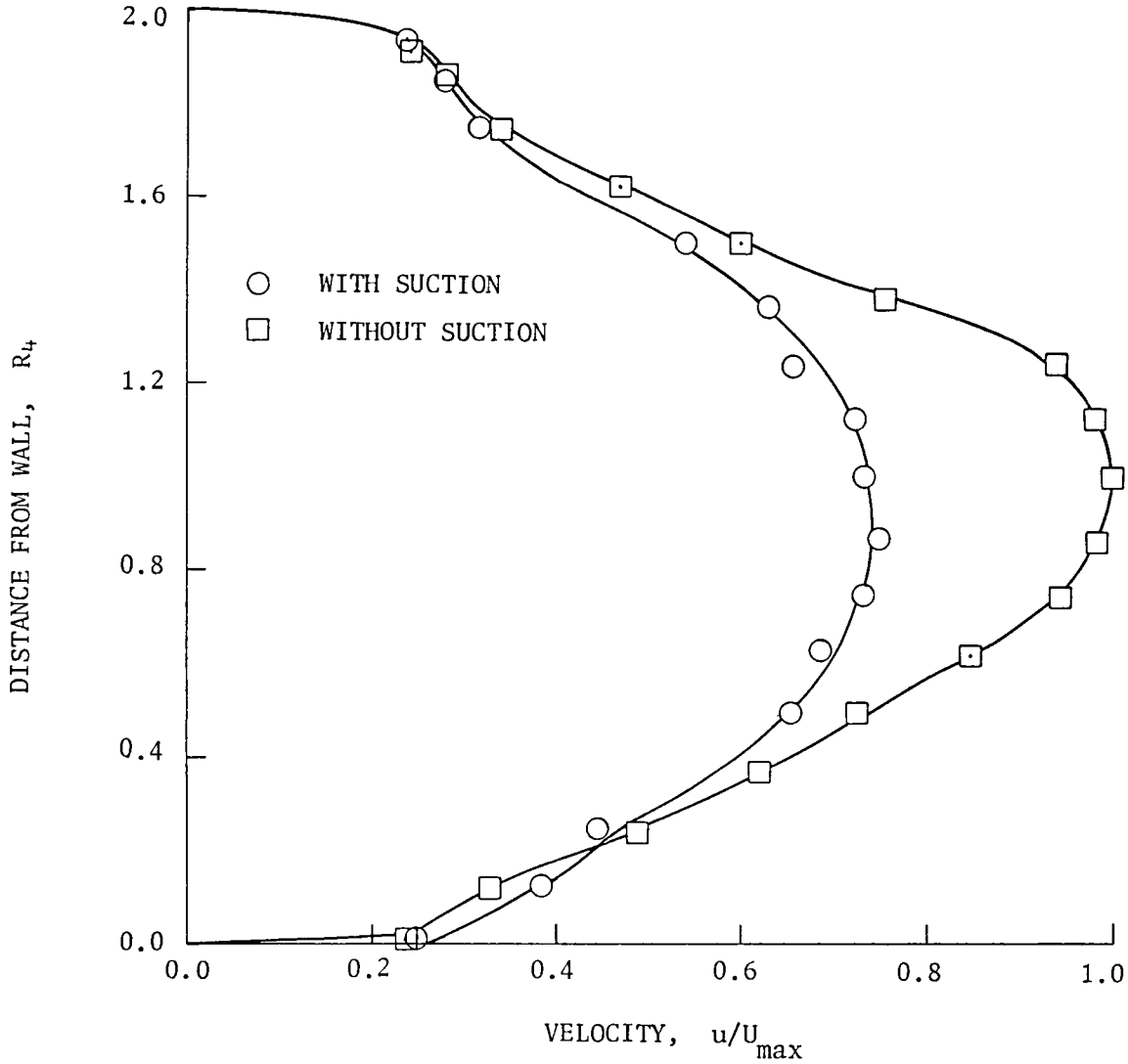

(a) Follower diffuser angle $2\theta = 10°$.

Figure 16. Velocity distribution with and without suction in the T_4 plane at exit from the follower diffuser; Reynolds number $R_e = 4.12 \times 10^5$; suction rate $q/Q = 0.095$; center velocity $U_{max} = 14.8$ m/s (48.4 ft/s).

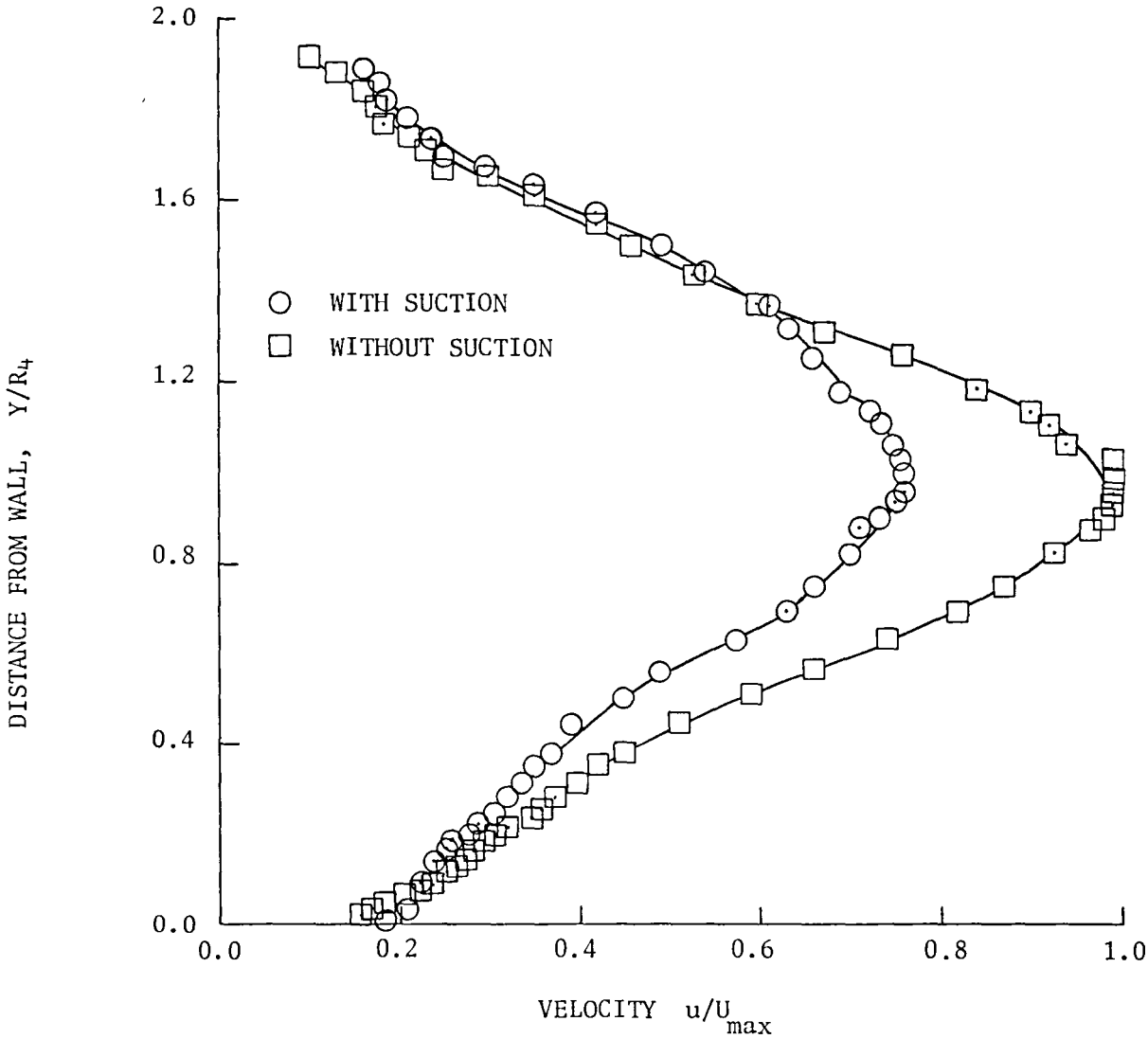

(b) Follower diffuser angle $2\theta = 20°$; Reynolds number $R_e = 6.12 \times 10^5$; suction rate $q/Q = 0.18$, center velocity $U_{max} = 19.1$ m/s (62.7 ft/s).

Figure 16. (Continued)

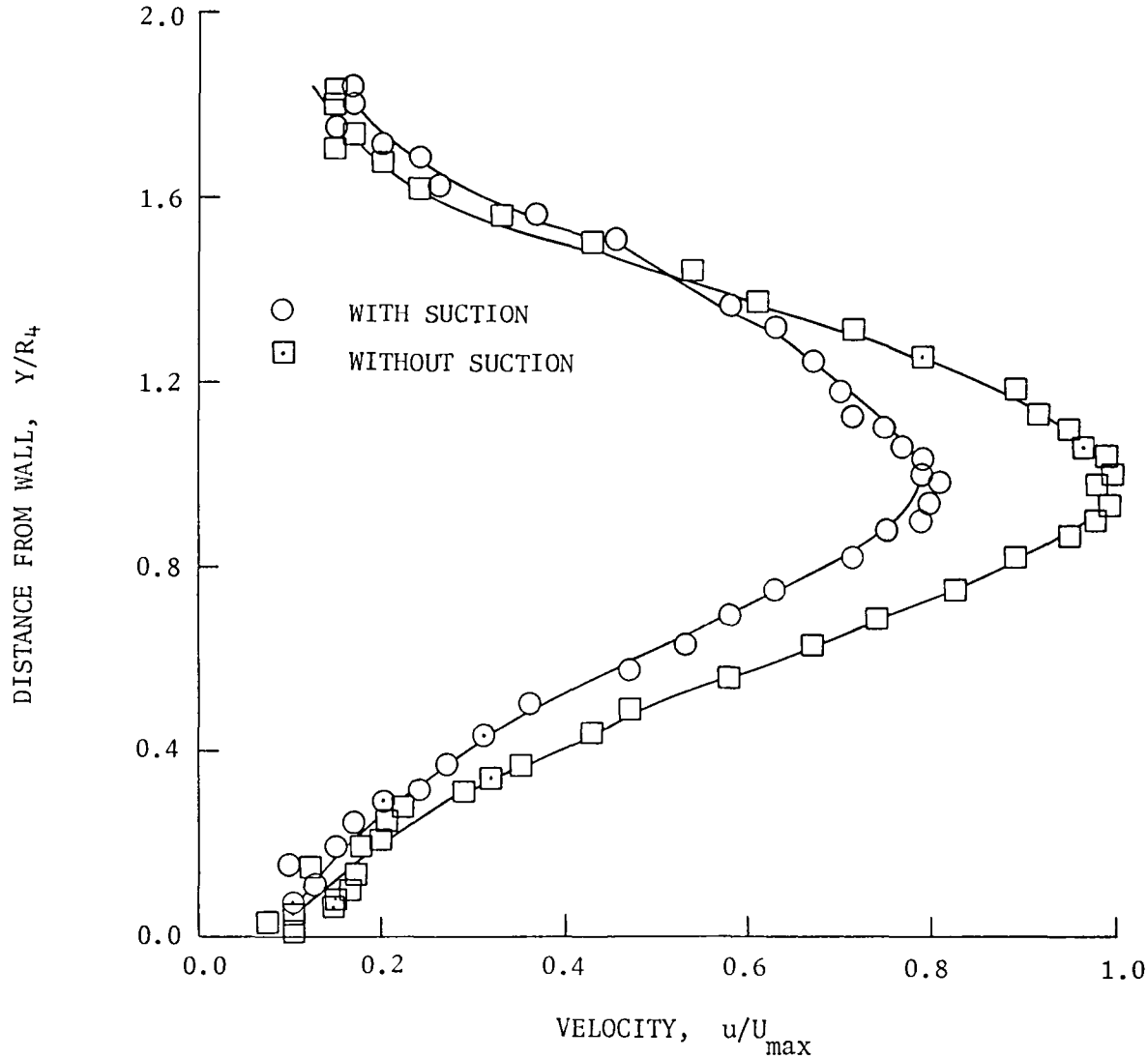

(c) Follower diffuser angle $2\theta = 30°$; Reynolds number $R_e = 6.12 \times 10^5$; suction rate $q/Q = 0.18$, center velocity $U_{max} = 23.7$ m/s (77.9 ft/s).

Figure 16. (Concluded)

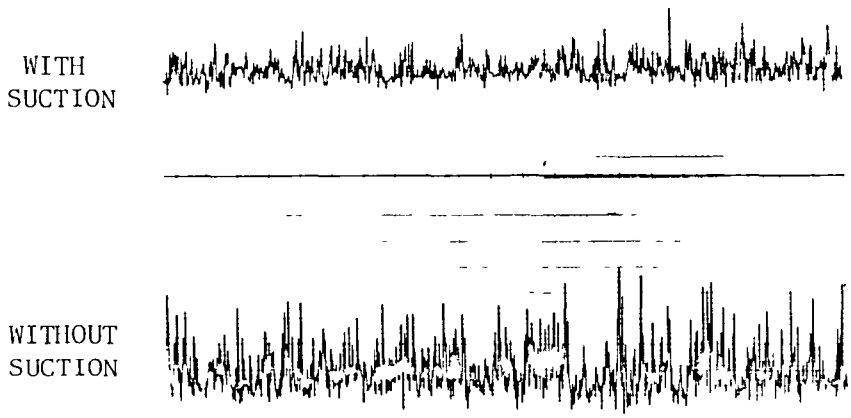

Figure 17. Velocity fluctuations at centerline with and without suction at exit from follower of 10° divergence angle, suction rate q/Q = 0.137.

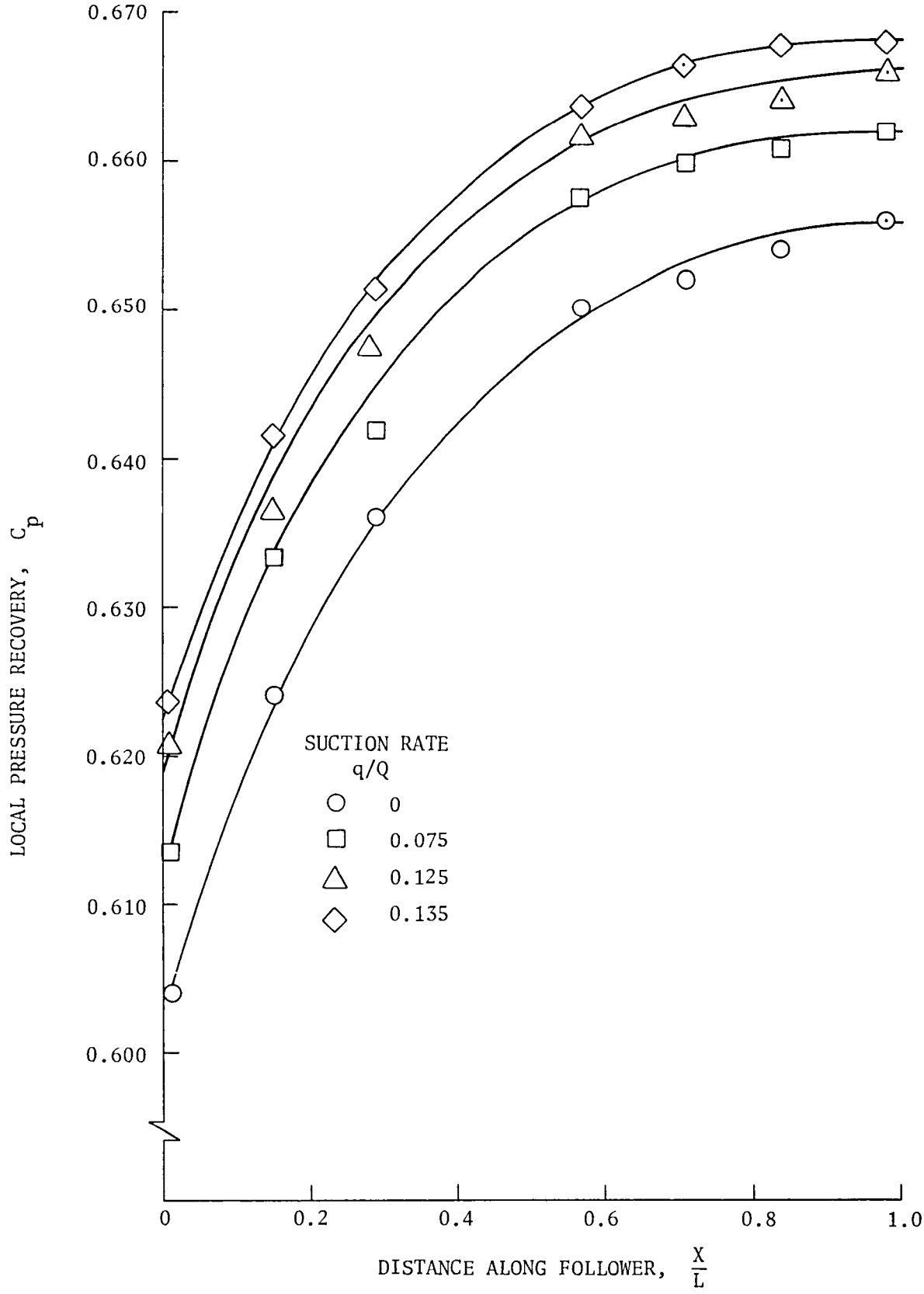

Figure 18. Local pressure recovery for various amounts of suction for the 10° follower diffuser at R_e = 6.1×10^5.

APPENDIX A

CALCULATION OF BLOCKAGE AT ENTRANCE TO LEADING DIFFUSER FROM EXPERIMENTALLY OBTAINED VELOCITY DISTRIBUTIONS

Let blockage

$$B = \frac{A_{geom} - A_{eff}}{A_{geom}}$$

where $A_{geom} = \pi R^2$ and $A_{eff} = A_{geom} - 2\pi R\delta^*$, δ^* being the displacement thickness of the boundary layer. For axisymmetric flow (See fig. A1):

$$U_c 2\pi R\delta^* = \int_o^R (U_c - u)\ 2\pi r dr$$

Introducing $r = R - y$, $dr = -dy$

$$\frac{\delta^*}{R} = \int_1^o \left(1 - \frac{u}{U_c}\right)\left(1 - \frac{y}{R}\right) d\left(\frac{y}{R}\right)$$

From the measured velocity distribution $u = f(y)$, the quantity $\left(1 - \frac{u}{U_c}\right)\left(1 - \frac{y}{R}\right)$ can be plotted against $\frac{y}{R}$ and integrated giving an area, say, A.

Hence $\delta^* = AR$ and $B = 2\pi R\delta^* = 2\pi R^2 A$. However, since blockage is expressed in percentage

$$B\% = \frac{B}{\pi R^2} = 2A$$

Therefore

$$B\% = 2\int_o^1 \left(1 - \frac{u}{U_c}\right)\left(1 - \frac{y}{R}\right)\ d\left(\frac{y}{R}\right)$$

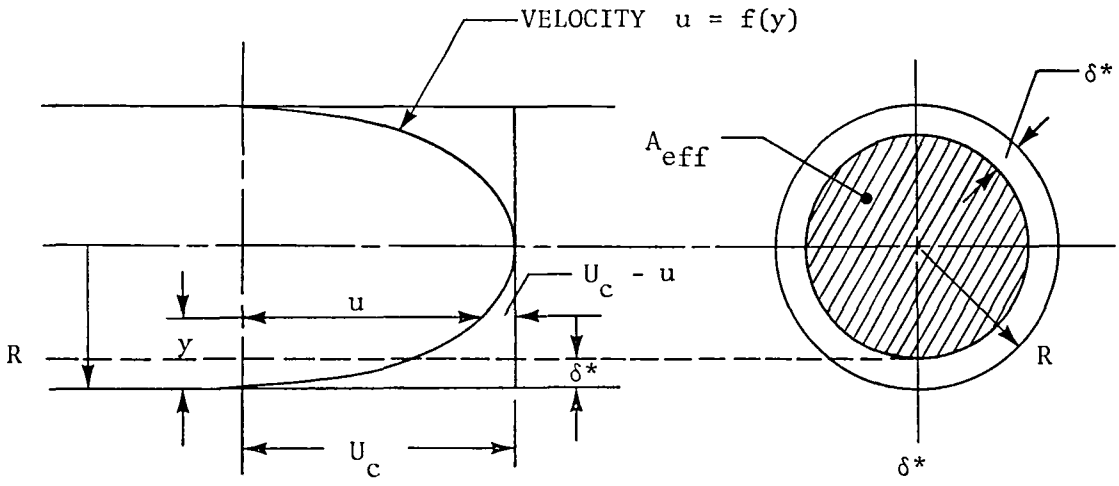

Figure A1.

APPENDIX B

CALCULATION OF THE SHAPE PARAMETER H

By definition

$$H = \frac{\delta^*}{\delta^{**}}$$

where δ^* is the boundary-layer displacement thickness and θ is the momentum thickness. From Appendix A

$$\frac{\delta^*}{R} = \int_o^1 \left(1 - \frac{u}{U_c}\right)\left(1 - \frac{y}{R}\right) d\left(\frac{y}{R}\right)$$

Similarly, momentum thickness may be defined as

$$U_c^2\, 2\pi R\theta = \int_o^R \rho u\, (U_c - u)\, 2\pi r dr$$

with $r = R - y$ and $dr = -dy$

$$\frac{\delta^{**}}{R} = \int_o^1 \frac{u}{U_c}\left(1 - \frac{u}{U_c}\right)\left(1 - \frac{y}{R}\right) d\left(\frac{y}{R}\right)$$

Hence the shape parameter

$$H = \frac{\delta^*}{\delta^{**}} = \frac{\int_o^1 \left(1 - \frac{u}{U_c}\right)\left(1 - \frac{y}{R}\right) d\left(\frac{y}{R}\right)}{\int_o^1 \frac{u}{U_c}\left(1 - \frac{u}{U_c}\right)\left(1 - \frac{y}{R}\right) d\left(\frac{y}{R}\right)}$$

REFERENCES

1. Yoshimasa, Furuya; and Kushida, Takehiro: The Loss of Flow in the Conical Diffusers with Suction at Entrance. Japan. Soc. Mech. Engrs. Bull., vol. 19, 1966.

2. Ackeret, J.: Removing Boundary Layer by Suction. NACA TM No. 395.

3. Juhasz, A.J.: Performance of an Axisymmetric Short Annular Diffuser with a Nondiverging Inner Wall Using Suction. NASA Technical Note D-7575, 1974.

4. Nelson, C.D.; and Hudson, W.G.: The Design and Performance of Axially Symmetrical Contoured Wall Diffusers Employing Boundary Layer Control. ASME 74-GT-152, 1974.

5. Yang, Tah-tec; Hudson, W.G.; and Nelson, C.D.· Design and Experimental Performance of Short Curved Wall Diffusers with Axial Symmetry Utilizing Slot Suction. NASA CR-2209, 1973.

6. Adkins, R.C.: Diffusers and Their Performance Improvement by Means of Boundary Layer Control. AGARD REPORT No. 654, June 1977.

7. Runstadler, P.W., Dolan, F.X.; and Dean, R.C.: Diffuser Data Book, "Creare Inc." Science and Technology, Hanover, New Hampshire, TN-186, May 1975.

1 Report No	2 Government Accession No	3 Recipient's Catalog No
CR-158957		

4 Title and Subtitle	5 Report Date
Experiments on Tandem Diffusers with Boundary-Layer Suction Applied in Between	February 1979
	6 Performing Organization Code
7 Author(s)	8 Performing Organization Report No
P. Stephen Barna	
	10 Work Unit No
9 Performing Organization Name and Address Old Dominion University Research Foundation P. O. Box 6369 Norfolk, Va. 23508	11 Contract or Grant No NAS1-14193-6 and NAS1-14193-42
12 Sponsoring Agency Name and Address National Aeronautics and Space Administration Washington, DC 20546	13 Type of Report and Period Covered Final Report Jan. 1, 1977-Jan. 1, 1978
	14 Sponsoring Agency Code

15 Supplementary Notes

This experimental work was funded under the Duct Acoustics Research Program of the Acoustics and Noise Reduction Division (ANRD) of NASA Langley Research Center for the exploration of flow fields of the Flow Duct Facility.

16 Abstract

Experiments were performed on conical diffusers of various configurations with the same, but rather unusually large, 16:1 area ratio. Because available performance data on diffusers fall short of very large area ratio configurations, an unconventional design, consisting of two diffusers following each other in tandem, was proposed. Both diffusers had the same area ratio of 4:1, but had different taper angles. While for the first diffuser (called "leading") the angle remained constant, for the second (called "follower"), the taper angle was stepped up to higher values. Boundary-layer control, by way of suction, was applied between the diffusers, and a single slot suction ring was inserted between them. The leading diffuser had an enclosed nominal divergence angle 2θ = 5 degrees, while the follower diffusers had either 10, 20, 30, or 40 degrees, respectively, giving 4 combinations.

The experiments were performed at four different Reynolds numbers and with various suction rates. The rates indicate a general improvement in the performance of all diffusers with boundary-layer suction. It appears that the improvement of the pressure recovery depends on both the Reynolds number and the suction rate, and the largest increase, 0 075, was found at the lowest R_e when the follower divergence was 2θ = 40 degrees. It also appears, however, that the rate of suction as compared with the flow rate through the diffuser must be relatively high; thus, the suction power necessary for effective improvements becomes also rather large, so that the benefit in improving diffuser performance by suction may be partly offset by power requirements.

17 Key Words (Suggested by Author(s))	18 Distribution Statement
Diffusers Reynolds number Boundary-layer control	Unclassified - Unlimited

19 Security Classif (of this report)	20 Security Classif (of this page)	21 No of Pages	22 Price*
Unclassified	Unclassified	55	$5.25

* For sale by the National Technical Information Service, Springfield Virginia 22161

End of Document